Silicon detectors for the upgrade of the HL-LHC experiments

Panagiotis Assiouras

National Center of Scientific Research Demokritos
Institute of Nuclear and Particle Physics
Detector Instrumentation Laboratory

Ph.D. presentation

Introduction

- Quality control:
  - Silicon sesnors before they are installed in the high energy experiments must have a substantial quality
  - CMS has developed a quality assurance plan to make sure that all the components meet the specifications.
  - Process quality control (contacted on dedicated test structures), together with the Sensor Quality control (contacted on the main sensors) consist of the two main procedures of the quality assurance of the sensors.
- Simulations:
  - Test structures like MOS, GCD and FET that are used in the PQC were simulated by using TCAD and compared with experimental results.
  - In addition, simulation of silicon sensor capacitance were performed by using TCAD simulations and a custom-made program, developed at the NSCR Demokritos
- Irradiation tests:
  - Irradiation studies of the electrical properties of test structures with gamma photons from a ^{60}Co source are presented along with the related TCAD simulations.

1. The HL-LHC and CMS Phase-2 upgrades
2. Quality control of silicon sensors
3. Simulation of silicon sensors and test structures
4. Irradiation tests with ^{60}Co source

From LHC to HL-LHC

- Phase-I: (2019-2021), Double the designed Luminosity: $2 \cdot 10^{34}\ cm^{-2}s^{-1}$, Integrated Luminosity: 300 fb^{-1} at Run 3.
- Phase-II: (2025-2027) , Luminosity: $5 \cdot 10^{34} cm^{-2}s^{-1}$, 300 fb^{-1} per year 3000 fb^{-1} for 10 years of operation

Figure: HL-LHC upgrade schedule.

Compact Muon Solenoid (CMS)

- CMS is one of two large general-purpose particle physics detectors built on the LHC at CERN.
- Consists of 4 sub-detectors:
  - Silicon Tracker: Designed to reconstruct trajectories of charged particles
  - Electromagnetic Calorimeter: Designed to measure with high accuracy the energies of electrons and photons.
  - Hadron Calorimeter: Designed to measure the energy of hadrons (protons, neutrons, pions and kaons)
  - Muon Chambers:Designed to identify muons and measure their momenta
- Current silicon Tracker will reach the end of its lifetime. Not expected to tolerate the increased radiation levels of HL-LHC
  - A lot of modules will be non-functional after 1000 fb^{-1} (first 3 years)

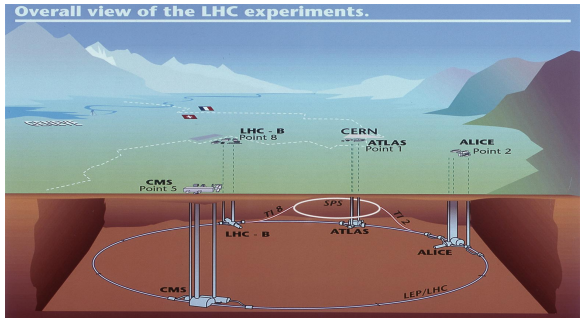

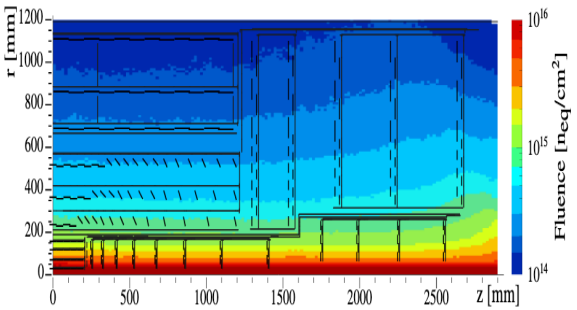

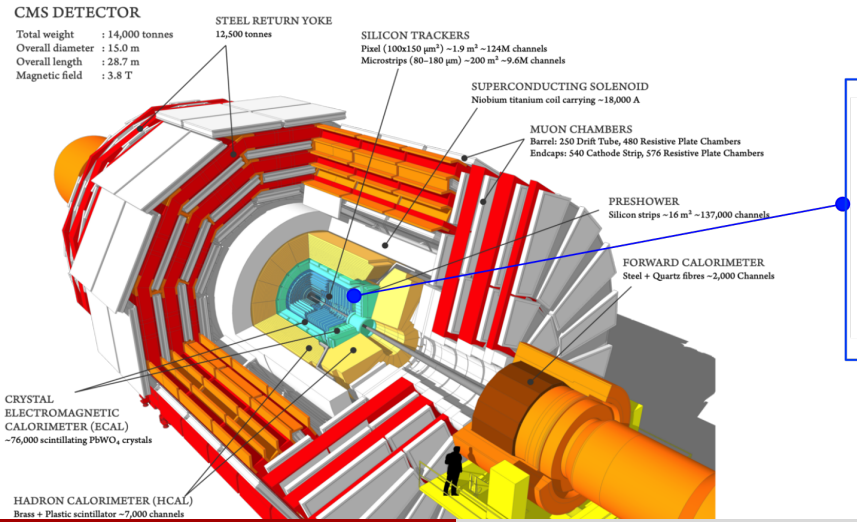

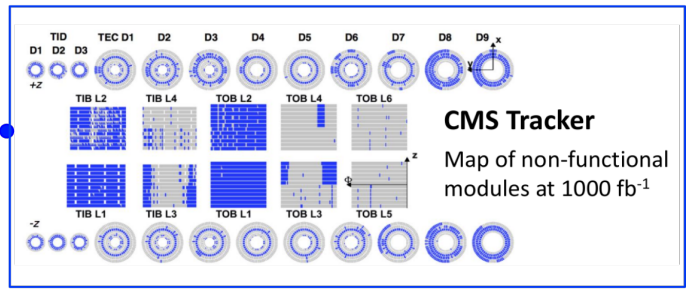

Total Replacement of CMS Silicon Tracker

- CMS tracking system will need a full replacement. The requirments for the upgrade are:

Radiation Tolerance up to $\int Ldt = 3000\ fb^{-1}$	Flip from p-on-n to n-on-p sensors, Oxygen-rich substrates
Pile Up 140-200, Occupancy < 1 %	Increase granularity, x20 more channels, Fully digital read-out
Longer Latency : from 3.2 μs to 12.5 μs	Increase front end buffer depth
Increase forward acceptance	Mostly through Pixel Detector extension up to |η|=4
Improve CMS Trigger	Contribution to Level-1 Trigger system: new modules with selective readout capabilities at 40 MHz
Improve resolution at low p_t	Reduce material: New geometry, Fewer layers/light material, new CO_2 cooling system
Improve resolution at high p_t	Increase granularity

Phase 1 Tracker

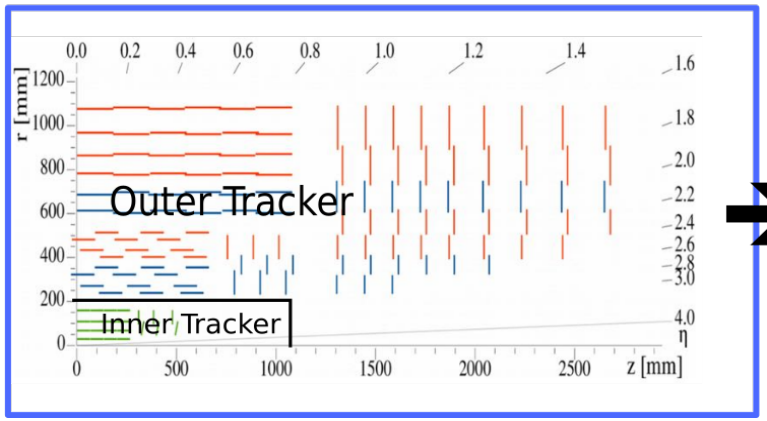

Phase 2 Tracker

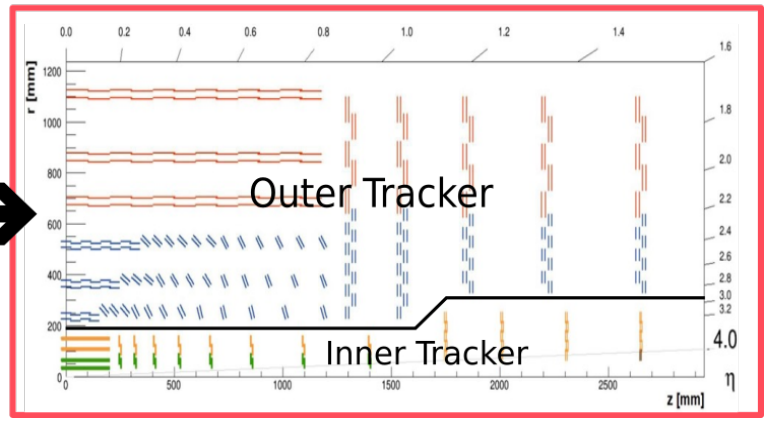

Contribution to the level-1 trigger: P_T modules

- New modules are needed capable of performing a discrimination of low p_T events ($p_T < 2$ GeV) at module level at bunch crossing rate.
  - Correlation of signals with a common read-out ASIC with programmable acceptance window
  - Reduce data volume sent to L1.
  - Keeping the most interesting events for physics studies
- Two parallel - closely spaced sensors:
  - 2S modules with two strip sensors
  - PS modules with one macro-pixel (PS-p) and one micro-strip (PS-s) sensors

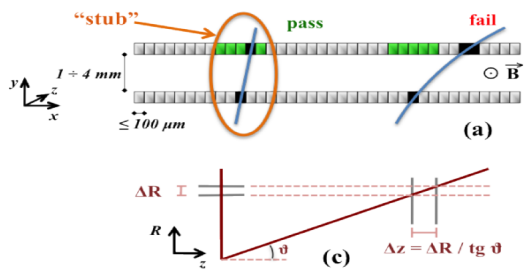

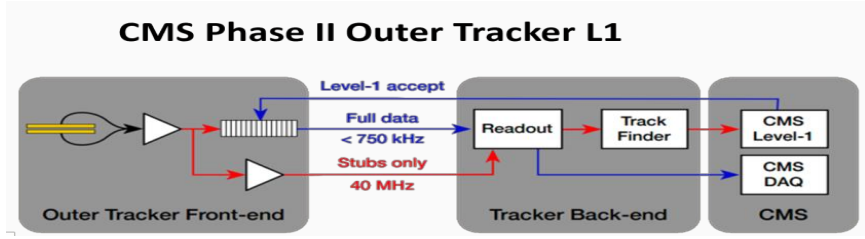

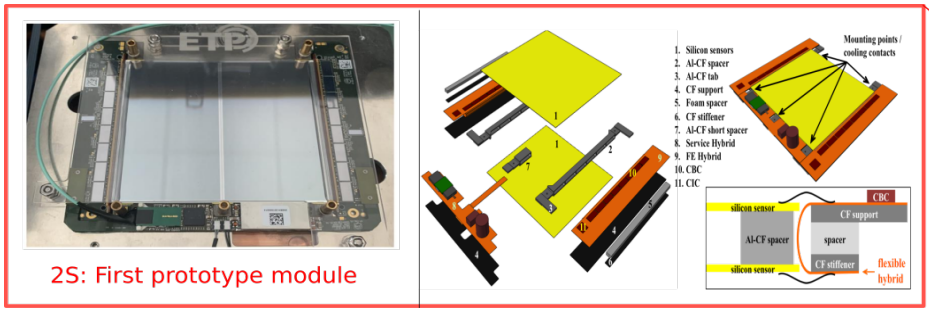

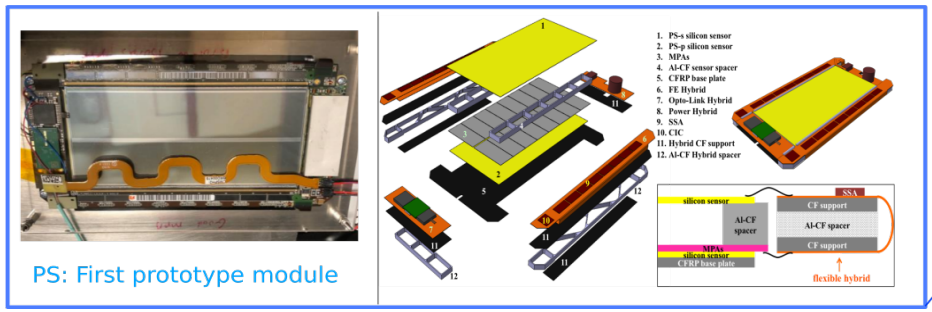

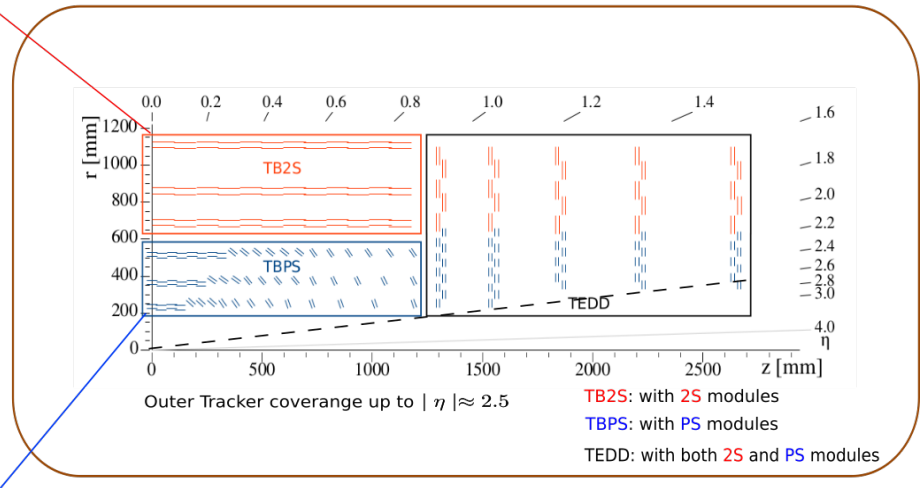

Outer Tracker sensors: Final design

Outer Tracker will encompass 200 m^2
Consisting of 24000 sensors
Two different modules with three different sensors

- 2S sensors: $6''$ wafers, FZ n-on-p, Act. thick. 290 um, AC coupled
- PS-s sensors: $6''$ wafers, FZ n-on-p, Act. thick. 290 um, AC coupled
- PS-p sensors: $6''$ wafers, FZ n-on-p, Act. thick. 290 um, DC coupled

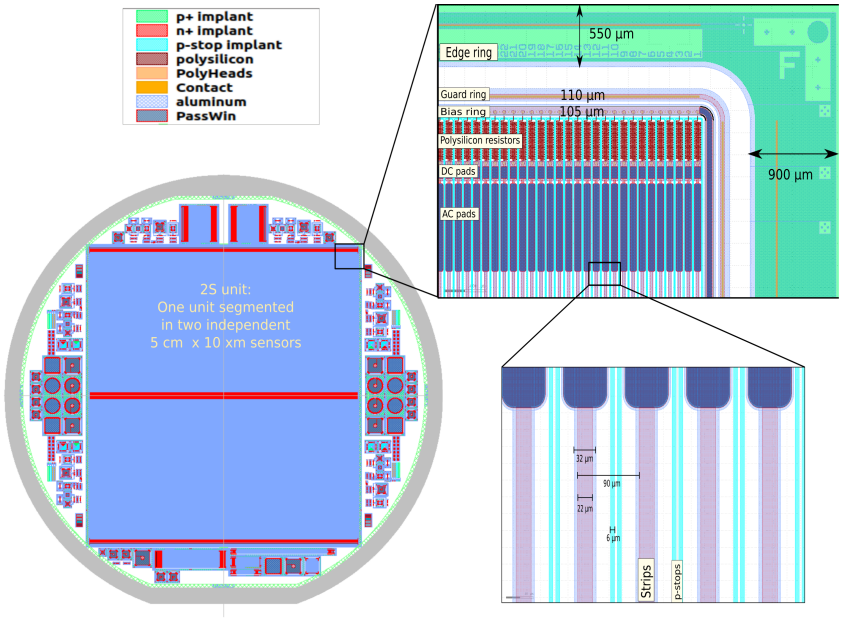

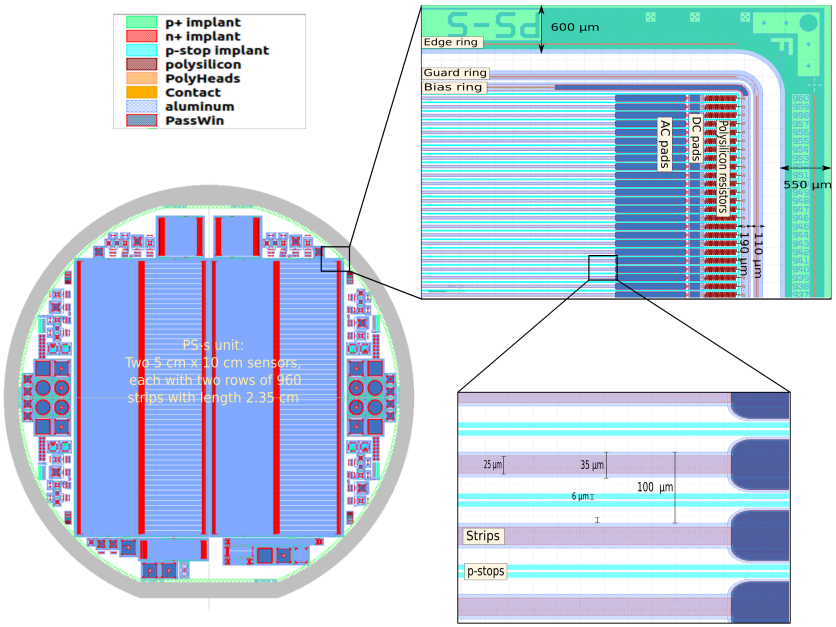

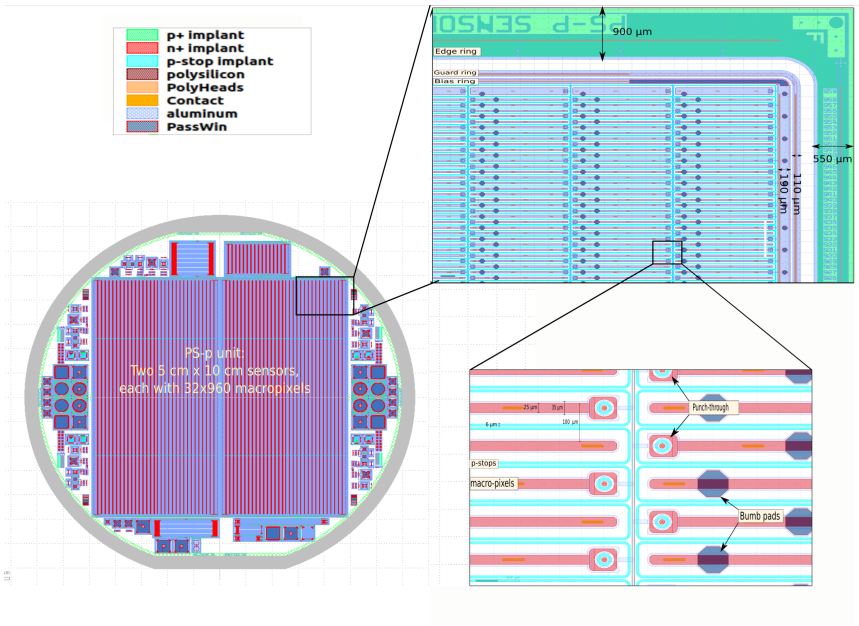

Quality control

Sensor and process quality control

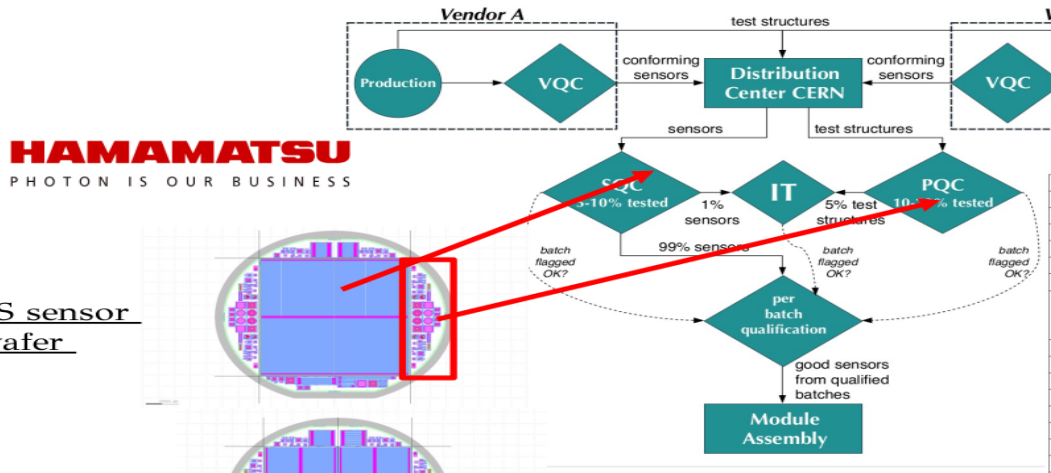

Parameter	Limit	Typical
Diode full depletion voltage V_{fd}	< 350 V	300 V
Current @600V I_{600}	≤ 2.5 nA/mm^3	
Flatband voltage $\|V_{fb}\|$	< 5 V	1.3-1.5 V
Oxide capacitance (oxide thickness)		700 nm
Surface recombination velocity s_0		0.6 cm/s
Thin oxide thickness (capacitance) C_{AC}	>1.2pF cm^{-1} pF^{-1} µm^{-1}	
Sheet resistances (metal, n+, p+, p-stop, poly silicon)		
Strip implant R_{strip}	< 250 Ω/square	32-35 Ω/square
Aluminium strip R_{alu}	< 30 mΩ/square	
p-stop implant $R_{p\text{-}stop}$		18-20 kΩ/square
p$^+$implant R_{p+}		
Polysilicon R_{poly}		2.2-2.4 kΩ/square
Bulk resistivity	> 3.5 kΩcm	3.5-8 kΩcm
Bulk doping concentration		
FET Threshold Voltage V_{TH}		2 V
Dielectric breakdown V_{diel}	> 150 V	
Linewidth (metal, n+, p+, p-stop, poly silicon)		ΔW_{n+}=4 µm? ΔW_{poly}=0.5 µm

- Sensor quality control
  - Direct measurement of subset of sensors which will be made into modules
  - Directly verify that HPK is producing sensors within our specs
  - Takes a lot of time. Less samples in the same batch can be measured.
- Irradiation tests
  - Irradiate mini sensors and test structures from same wafer as diced sensors
  - Verify that the silicon will behave within spec after expected radiation doses of HL-LHC
- Process quality control
  - Measurement of test structures located on the same wafer constructed with the same properties as the main sensors, utilizing the empty space on the edges of the wafers.
  - Verify silicon quality without the need to handle sensors
  - Takes less time. More samples in the same batch can be measured

QA centers

- SQC centers
  - Brown University (USA)
  - University of Delhi (India)
  - Institute of High Energy Physics in Vienna (Austria)
  - Karlsruhe Institute of Technology (Germany)
  - NCP (Pakistan)
  - Rochester Institute of Tech- nology (USA)
- PQC centers
  - Brown University (USA)
  - NCSR ”Demokritos”(Greece)
  - Institute of High Energy Physics in Vienna (Austria)
  - INFN Perugia (Italy)
- IT centers
  - Karlsruhe Institute of Technology (Germany)
  - Brown University (USA)

- Sensor production started since summer of 2020 and will run until the mid 2024.
- More than 12000 wafers (≈ 50 %) have been tested so far.

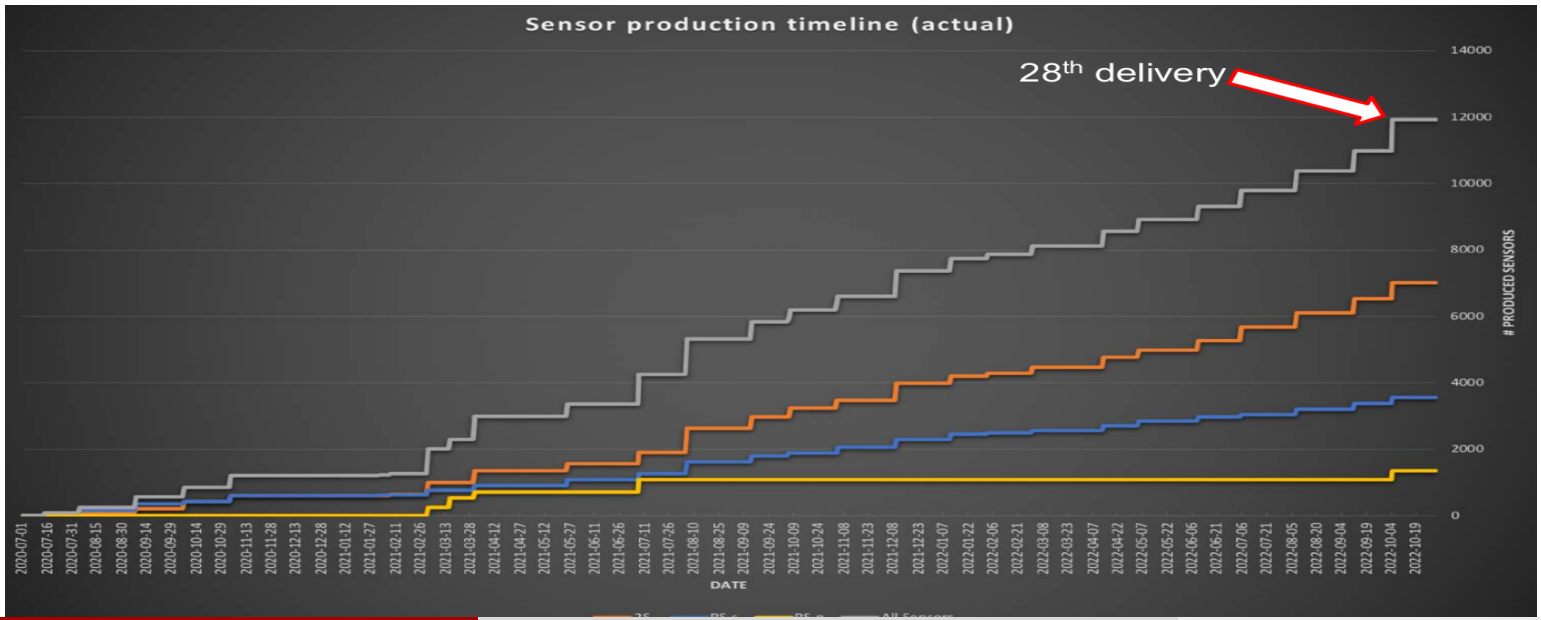

PQC mesurments: Flute structures

- Test structures that are arranged around an array of 20 contact pads, called ”flute”
  - Automated measurements by using a 20 needle probe card and a switching matrix

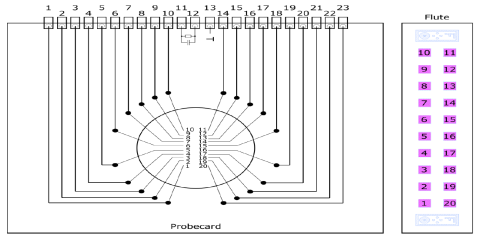

- Each Half Moon contains 2 sets of 4 flutes in each side. They are seperated in
  - Quick Flutes (Quick evaluation of most important parameters. Takes about 30 min)
    - Flute 1: MOS, Van der Pauw structures (P-stop, n+, Poly), FET
    - Flute 2: GCD, Rpoly, Diel Breakdown, Linewidth(n+, p-stop)
  - Extended Flutes (Providing additional parameters. Performed in a smaller number of wafers. Takes about 50 min)
    - Flute 3: Diodes Half, VDP(Bulk, Edge(p+), Metal(Al))
    - Flute 4: GCD05, Cross bridge kelvin resistances (n+, Poly)
  - Additional flute and standard test structures to be contacted with needles.

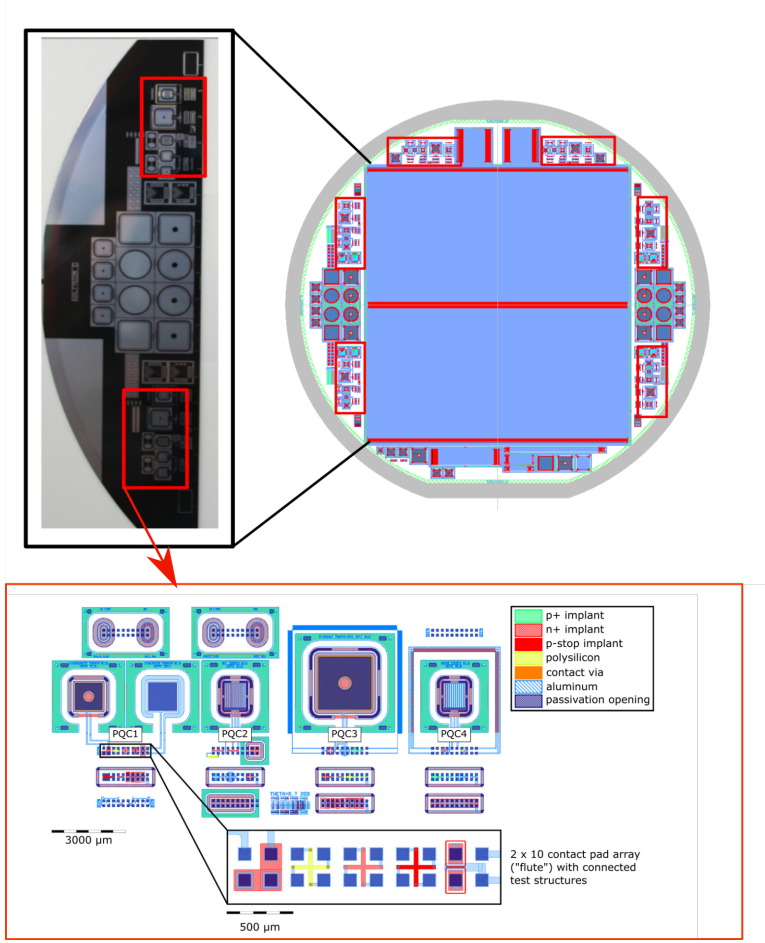

Experimental setup at NCSR "DEMOKRITOS" lab

- Electrical characterization setup consisting of:
  - Probe Station: Karl Suss PA 150
  - CV: HP4092A
  - IV: Keithley 6517A
  - IV: Keithley 2410A
  - The whole setup is controlled with a LabView program
  - A probe card and switching matrix is used for automated of the measurements on the flute structures
- Enviromental conditions are constantly monitored:
  - Relative humidity < 30 % RH
  - Temperature fixed at 20 ^{o}C
- PQC measurement results are initially written to ASCII files and stored at the PQC station computer.
- The analysis of all measurements is performed with Python and ROOT scripts
- The measurements along with the analysis results are covrerted are submitted to the database in the form of XML-files.

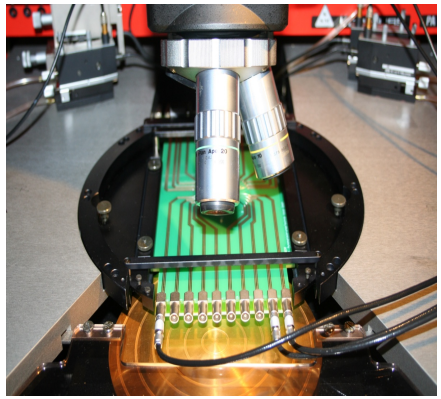

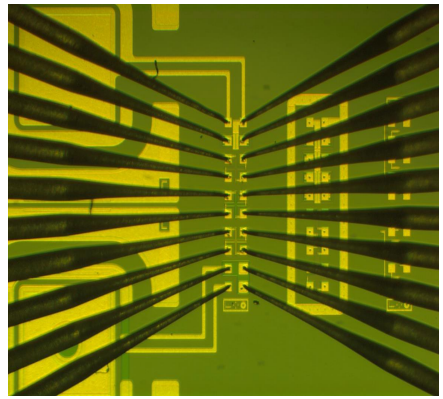

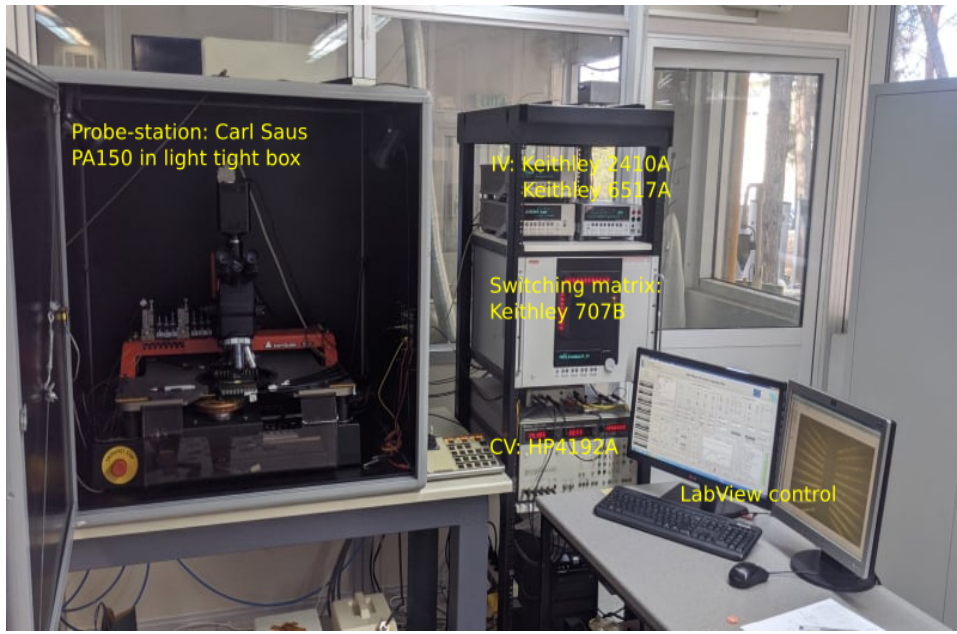

Van der Pauw cross structures

- Van Der Pauw (VDP) test structures are used to measure the resistance of thin films (Al, n+, p-stop, Edge)
- A current source is applied in two contacts. The voltage difference is measured to the other two contacts

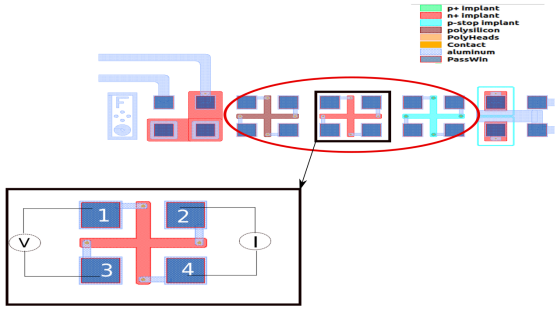

$$R_{sh} = \frac{\pi}{ln(2)} \frac{V}{I}$$

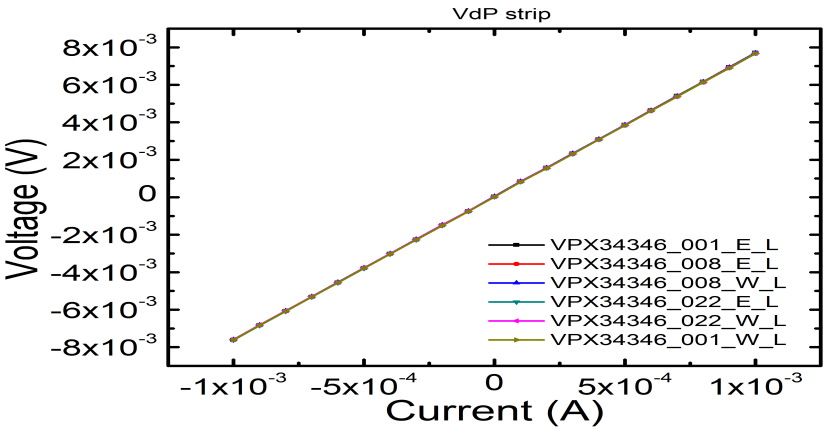

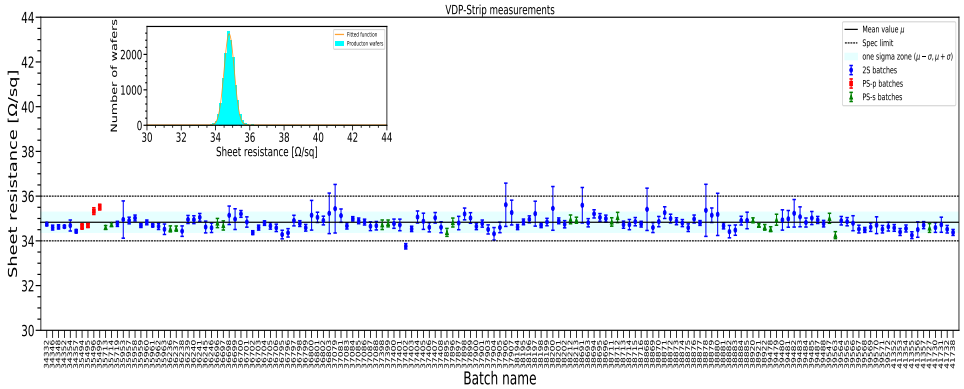

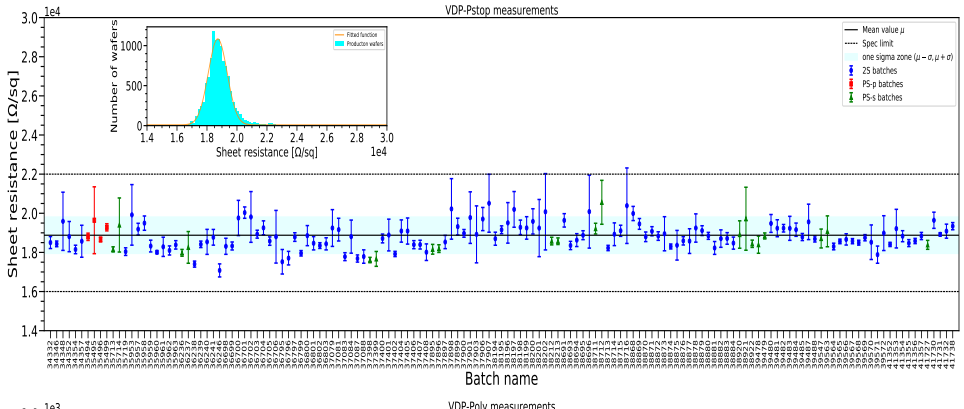

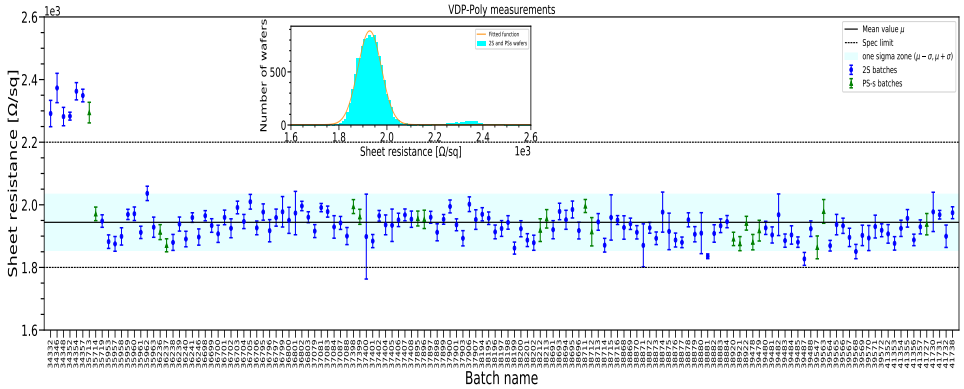

Metal Oxide Semiconductor capacitors (MOS)

- MOS capacitor is the most useful device in the study of semiconductor surfaces and interfaces.

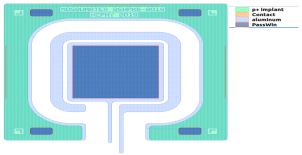

- Parameters measured with this device:
  - Flatband voltage $V_{fb} = \phi_{Al} - \phi_{Si}$
    - Ideal case: $V_{fb} = 0$
    - Non ideal: $V_{fb} \propto N_{ox}$
  - Fixed oxide charge concentration N_{ox}
  - Oxide capacitance C_{ox}
  - Oxide thickness $t_{ox} = C_{ox}/\varepsilon_{Si}A$

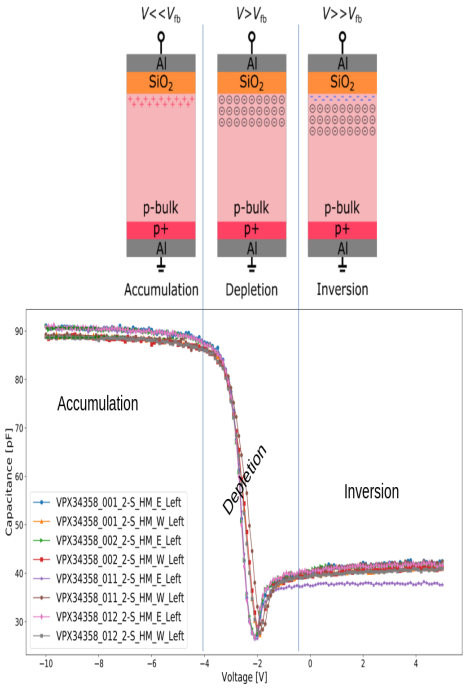

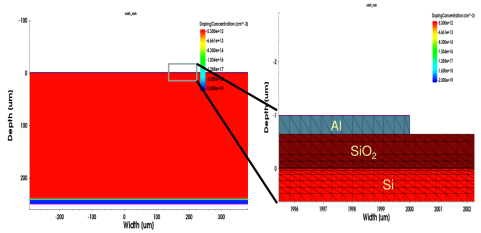

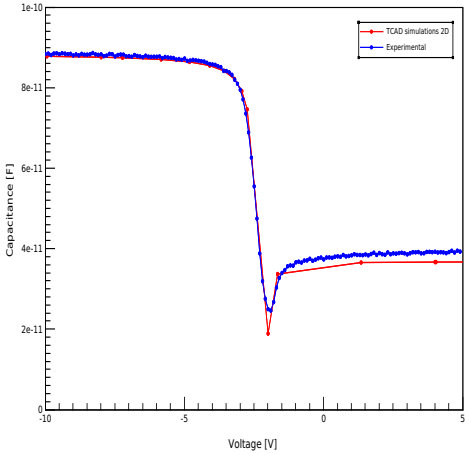

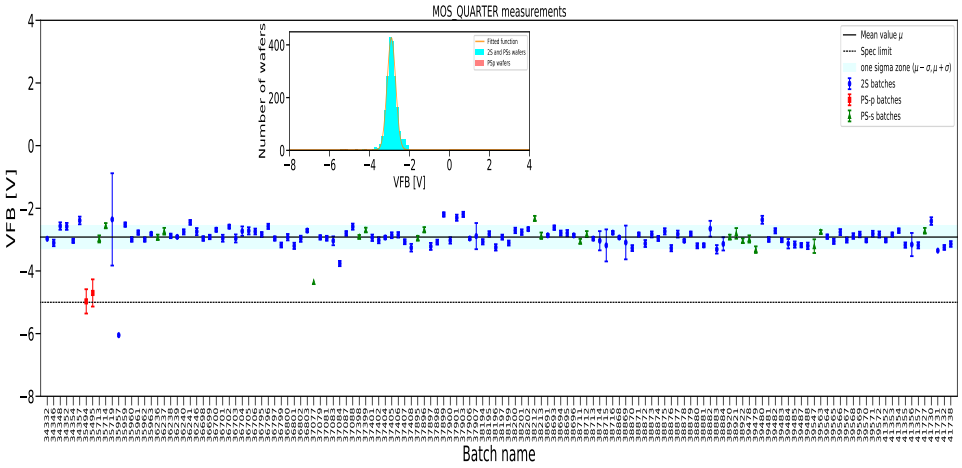

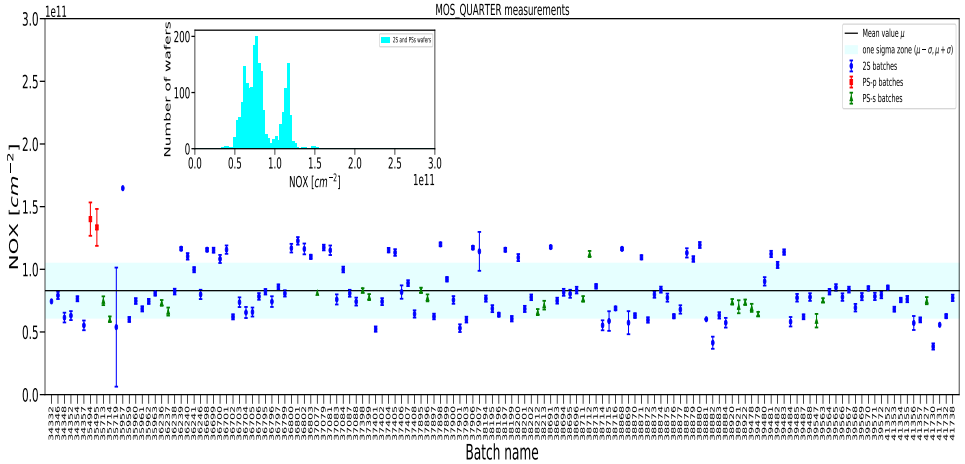

Gate controlled diodes

- GCDs are used to investigate the surface current and the number of interface traps
- Consisting of comb-shaped Diode with n+ strips, intertwined with comb-shaped MOS.

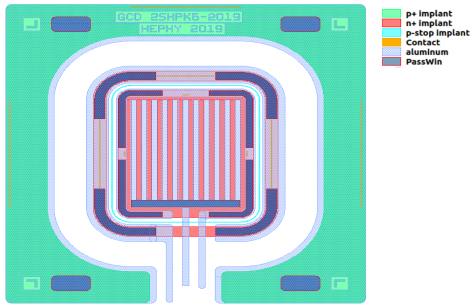

- Parameters measured with this device:
  - Surface current $I_{surf} = I_{depl} - I_{inv}$
  - Surface recombination velocity $S_0 \propto I_{surf}$
  - Interface trap density $D_{it} \propto S_0$

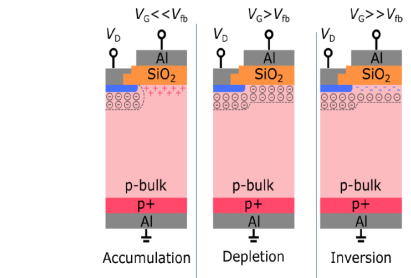

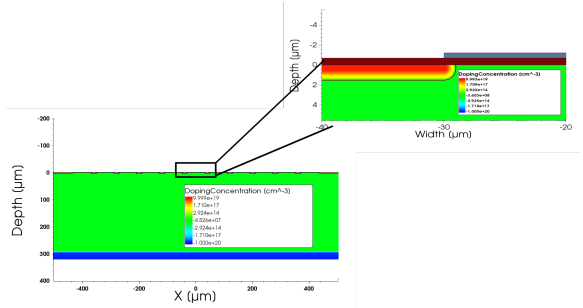

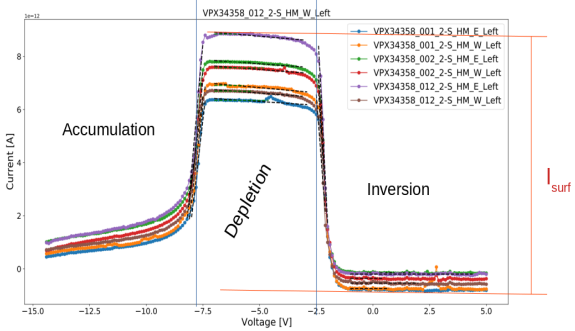

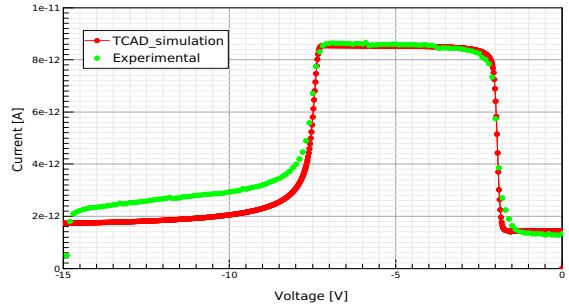

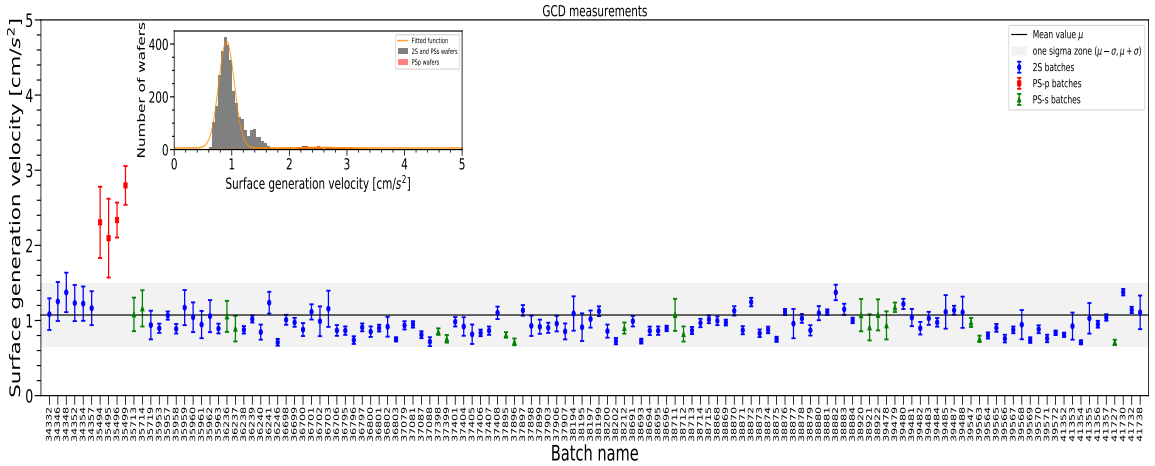

Field effect transistors

- Field-Effect Transistor (FET) test structures can be used to qualitatively determine the strip isolation quality and inter-strip resistance.

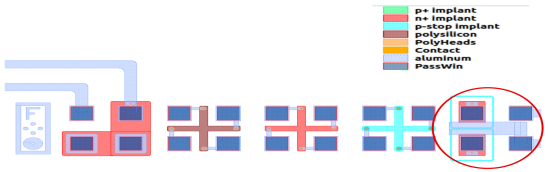

- The FET inter-channel region replicates the sensor inter-channel region:
  - The distance between the source and drain is equal the distance of two neighboring strips.
  - P-stop implants encircle source and drain with exactly the same properties as the sensor (the n+ implant distance, the p-stop layout, the p-stop doping).
- FET threshold voltage is sensitive to variations of p-stop and inter-channel properties and it can provide an evaluation of the p-stop quality.

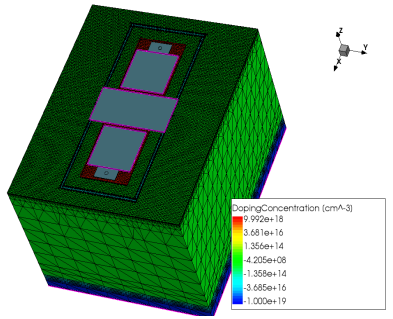

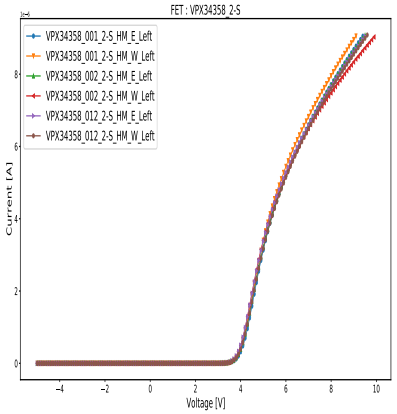

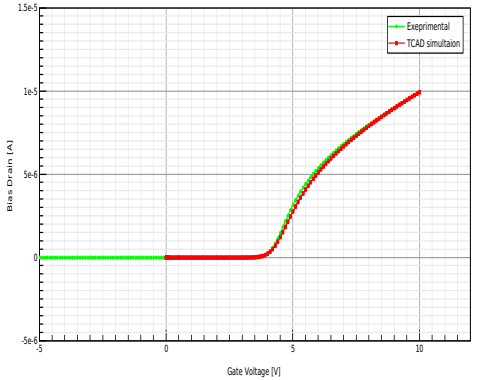

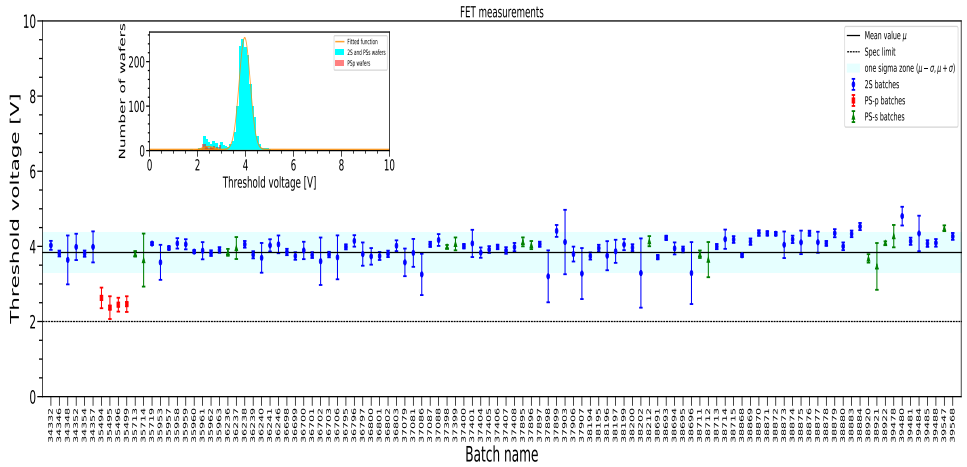

Minor issues: P-stop in-homogeneity

- n-on-p sensors are sensitive to the p-stop doping (implant dose and profiles). P-stop is responsible of the isolation of the strips.
- V_{th} and p-stop resistivity give a qualitative evaluation of the inter-strip isolation.
- Non-uniform measurements has been observed between East and West half-moons regarding the sheet resistance and threshold voltage.
  - Significant large non-uniformity across the wafer shows that there are instabilities in the process which has to be checked and monitored continuously.
- No interstrip resistance issues observed on the sensors from wafers with lower threshold voltages.
  - This indicates that the p-stop is still good enough or that this non-uniformity issue affects mostly the periphery.
- There are no indications that this would limit the lifetime of the sensors.
- Irradiation tests on these samples is on-going

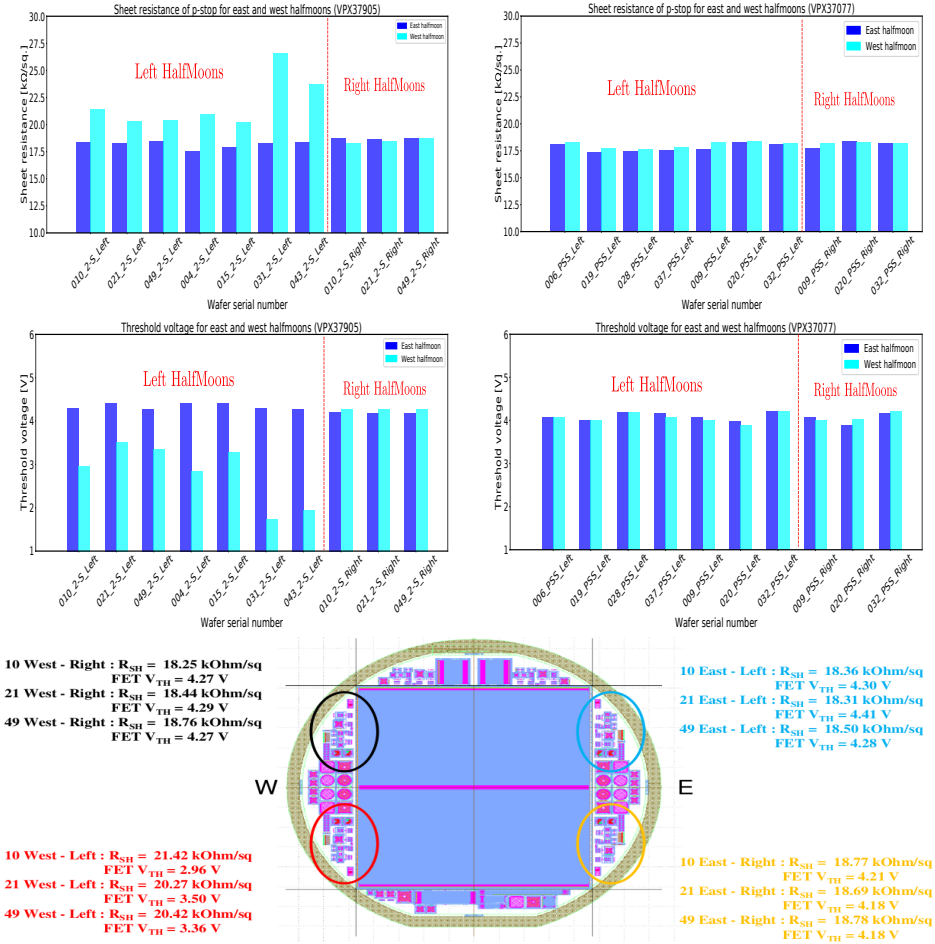

Summary on the Quality control

- The Process Quality Control (PQC) aims to monitor the stability of the sensor fabrication process.
- Delivered sensors by HPK show very good quality so far!
- All the batches that were tested so far were qualified as qood
  - Uniform measurements between different batches
  - Good agreement between the PQC centers
- Outer Tracker will be comprised with sensors of high quality for the HL-LHC era!

Simulation of silicon sensors and test structures

TCAD simulations: Test structures

- TCAD is used to provide a better insight of the complex phenomena related to semiconductor devices. It follows a finite element analysis scheme:
  - The device is designed in two or three dimensions. The doping concentrations and the geometry of each region are well defined
  - Then is subdivided to finite elements, which creates a mesh of the device
  - The desired physical models are defined. Such as: Shockley-Read-Hall recombination, avalanche electron-hole generation, doping dependence mobility..
  - The fundamental partial differential equations for semiconductors are solved.

$$\nabla \cdot (\epsilon \nabla V + \vec{P}) = -q(p - n + N_D - N_A) - \rho_{trap} \quad (1)$$

$$\nabla \cdot J_n = q(R_{net,n} - G_{net,n}) + q\frac{\partial n}{\partial t} \quad (2)$$

$$\nabla \cdot J_p = q(R_{net,p} - G_{net,p}) + q\frac{\partial p}{\partial t} \quad (3)$$

- Then the macroscopic factors can be calculated. Such the Capacitance and the Leakage Current of the device.

- FET structures

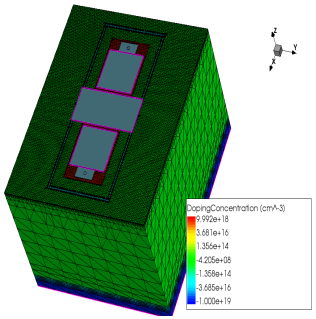

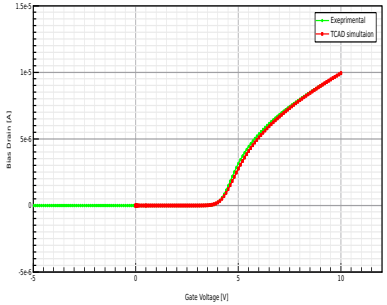

- MOS structures

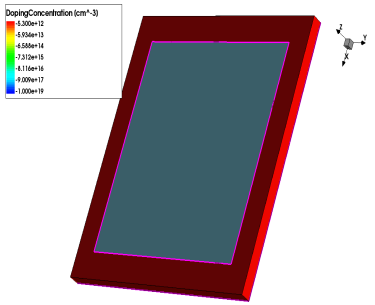

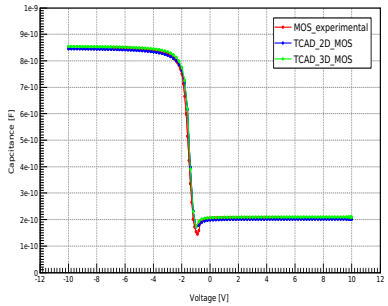

- Gate controlled diodes

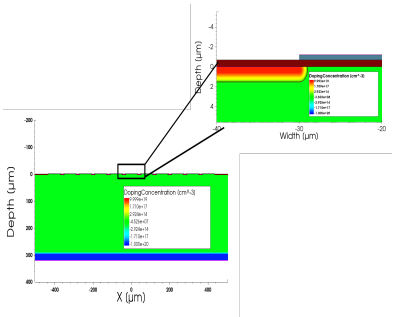

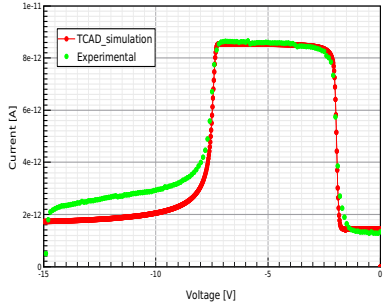

TCAD simulations: FET structures

- 3D structure that was used for the simulation of the MOSFET
- The middle metal pad is the gate, while the other two are the source and the drain which are connected with the implantation beneath the oxide.

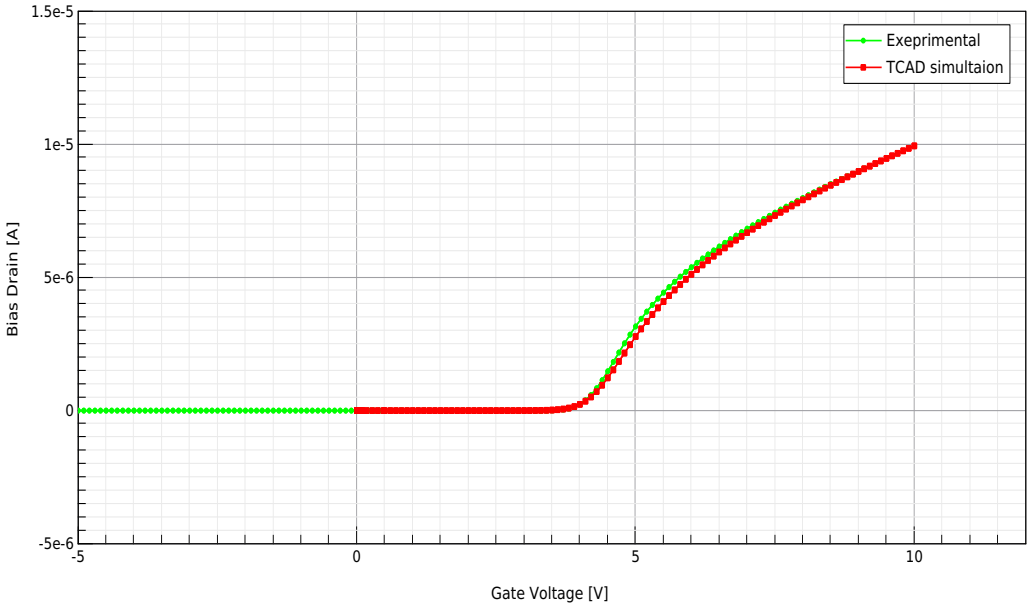

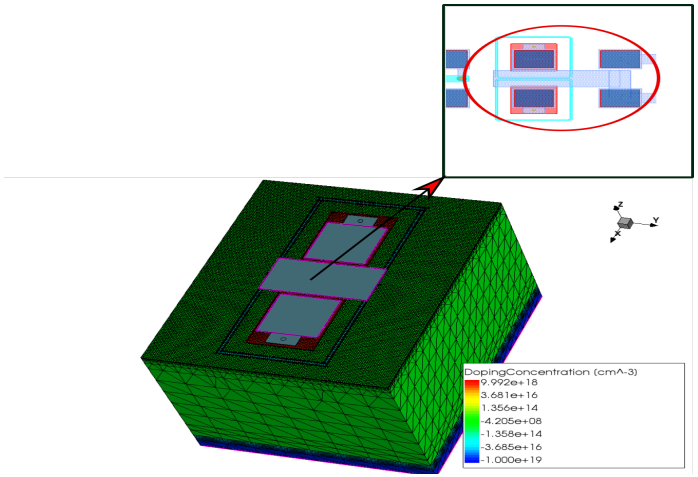

MOSFET thickness	330 μm
Backplane thickness	30 μm
N_{bulk}	4.0×10^{12} cm^{-3}
Oxide thickness	0.65 μm
Aluminum thickness	1.0 μm
Implant thickness	1.5 μm
Implant doping	1.0×10^{19} cm^{-3}
p-stop doping	1.0×10^{16} cm^{-3}
N_{ox}	5.64×10^{10} cm^{-2}

Table: Geometrical properties and doping concentration used for the TCAD simulation of the MOSFET

Simulation of capacitances with a 3D and 2D numerical solution of the Laplace's equation.

- We have developed a software for fast estimation of capacitances in planar silicon pixel and strip sensors based on a numerical solution of the Laplace equation
- Some key aspects of the program:
  - It solves the Laplace equation in 2D for the strip case 3D for the pixel.
  - The axis that is parrallel to the junction plane is diacritized to finite elements.
  - By performing a Fourier Transform it reduces the problem by one dimension
  - The problem is solved in the Fourier space by using a numerical algorithm.
- *Advantage*: Calculation time of about some seconds
- *Disadvantage*: Not a very detailed simulation.
- Comparison with TCAD simulations and experimental measurments performed on the MSSD sensors for the strip sensors. For pixel sensors the comparison was made only with TCAD simulations and experimental data that was found in literatutre. More details can be found in [1]

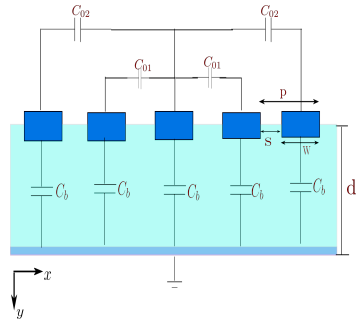

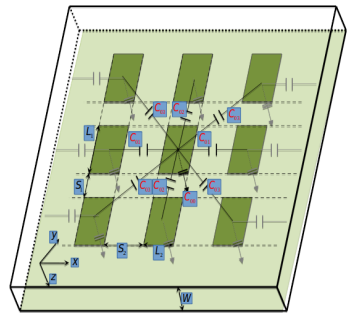

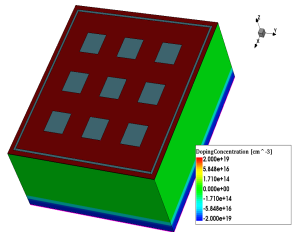

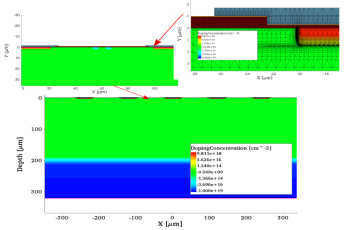

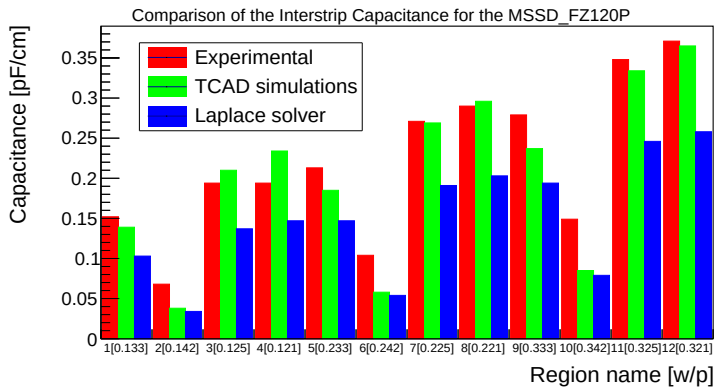

[1] P. Assiouras, et al, Journal of Instrumentation, 15(11):P11034–P11034,

Calculation of capacitances of Outer Tracker sensors: with Laplace solver

- We have calculated the capacitances of the sensors of Outer Tracker by using both the simulation program developed at Demokritos and TCAD ($ENC \propto C_d$)
- The capacitances are calculated for fixed strip and pixel geometry and various sensors thickness.

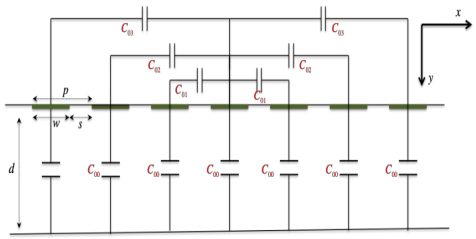

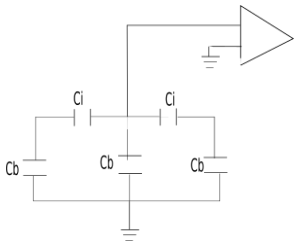

- 2S sensor:

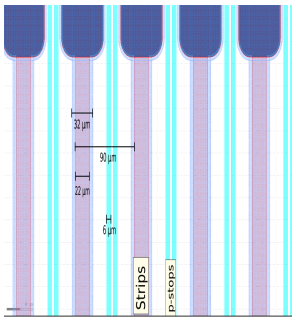

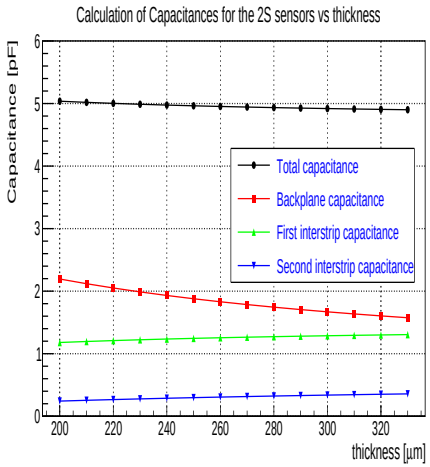

- PSs sensor:

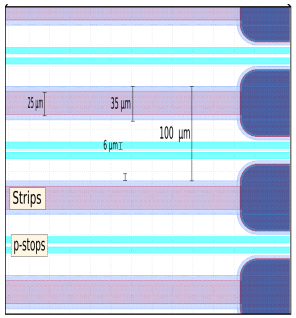

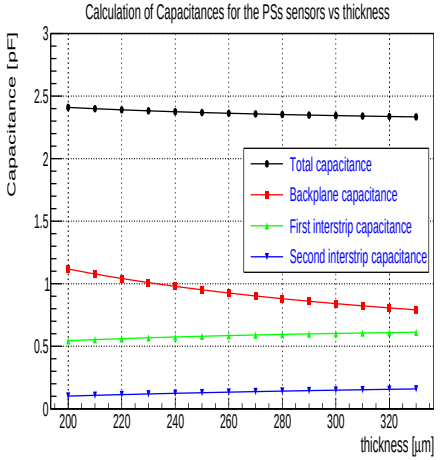

- PSp sensor:

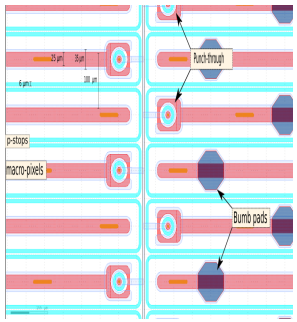

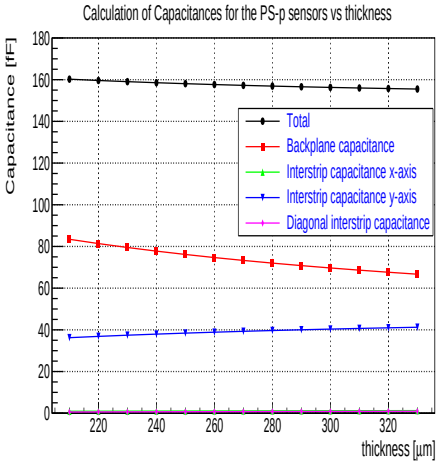

TCAD simulations of interstrip and interpixel capacitance

- For the 2S and PS-s: a 2D structure was used consisting of 5 stips with an n^+p configuration
- For the PSp sensors: a 3D structure was used consisting of 9 pixels with an n^+p configuration

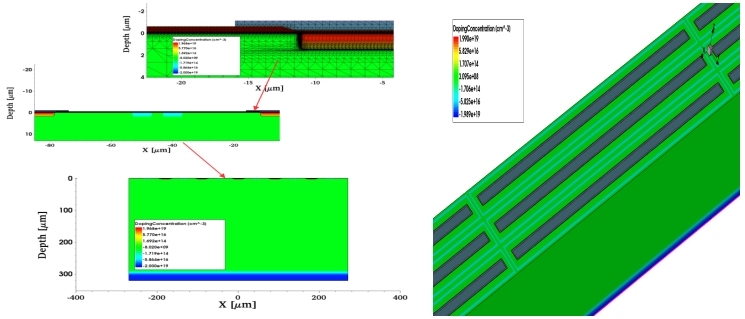

- 2S sensors: Comparison with SQC data uploaded to database

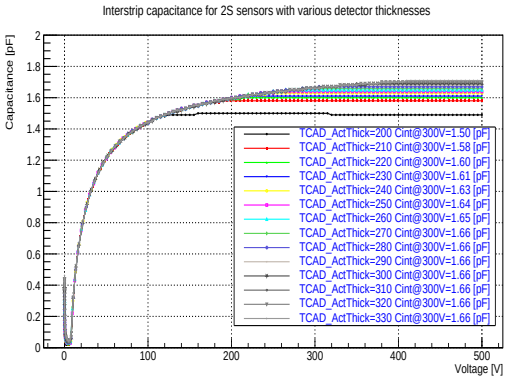

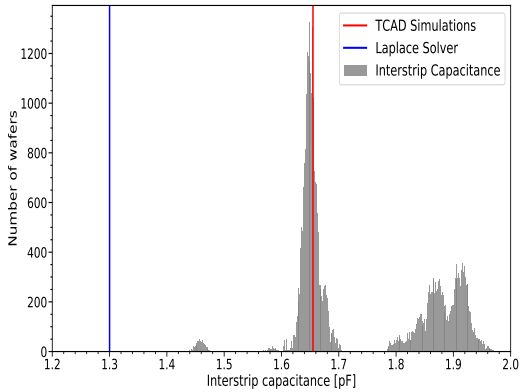

- PSp sensors: Comparison with measurements performed at KIT

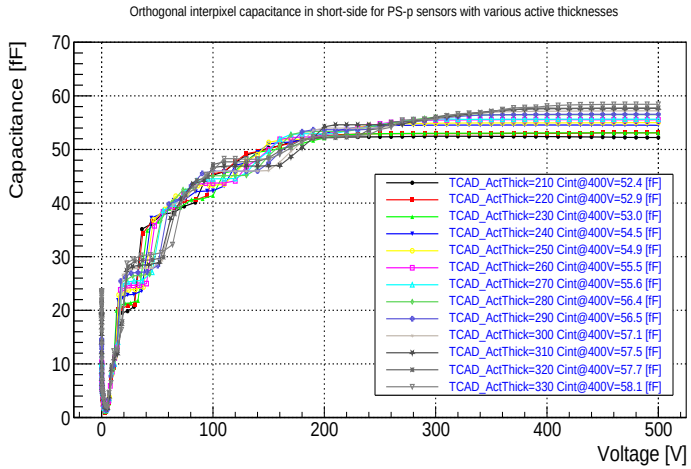

- PSs sensors: Comparison with SQC data uploaded to database

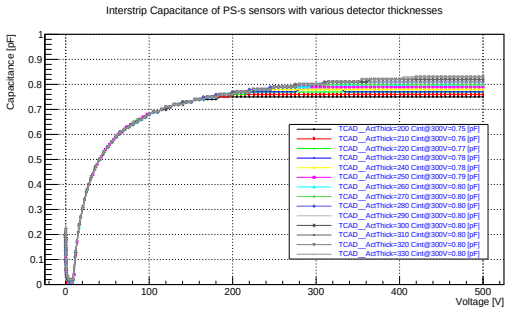

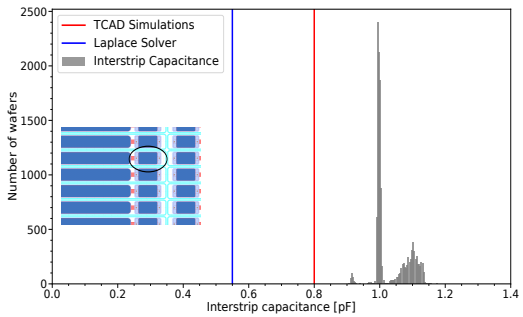

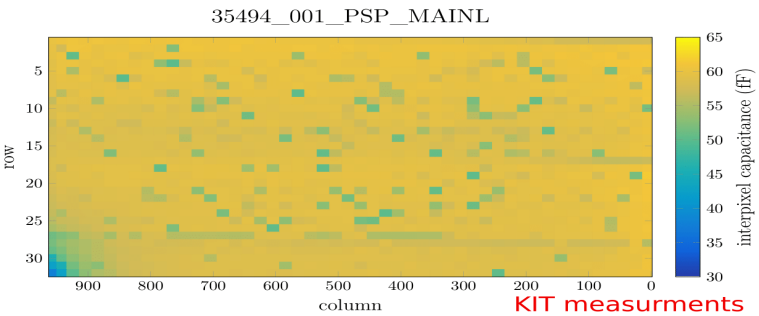

Summary on simulations

- Test structures like MOS, GCD and FET that are used in the PQC were simulated by using TCAD and compared with experimental results.
- In addition simulation of silicon sensors capacitances were performed by using TCAD and also by an in house developed 3D Laplace solver algorithm.
- The validity of the custom made program was checked, by comparing the results with TCAD simulations and experimental data.
- Both TCAD simulations and our custom-made simulation program were used for simulating the silicon sensor capacitances (backplane, interstrip and interpixel) of the OT sensors.
- The experimental SQC results are corroborated by the simulations with very good agreement.

Irradiation studies by using a ^{60}Co source

Radiation damage on silicon sensors

There are two kinds of radiation damage:

- Bulk damage
  - Caused mostly by hadrons
  - Formation of vacancies V and interstitials I, or more complex defects (VO, V_2, VP)
  - Macroscopic effects: increase of leakage current, decrease of charge collection efficiency, increase of full depletion voltage
- Surface damage
  - There are two major families of defects, some pre-exist from fabrication and some are produced (or activated) from radiation
    - Fixed oxide charges: (E′ centers), located near the interface, formed when a O_2 atom is missing
    - Interface traps: (P_b centers), located in the interface where the lattice is highly distorted
  - Ionizing radiation generates e/h pairs in the SiO_2
    - e^- move rapidly towards the gate (only a small percent are trapped in the oxide)
    - h^+ move more slowly towards the interface (polaron hopping)
    - Some h^+ can be trapped by the E′ centers and some can be trapped by the P_b centers.
    - Macroscopic effects: increase of flat-band, decrease of interstrip resistance, increase interstrip capacitance

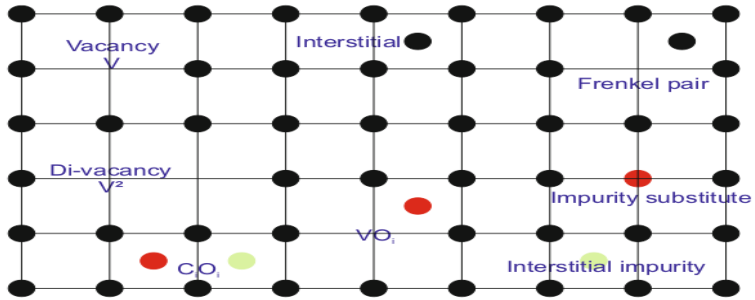

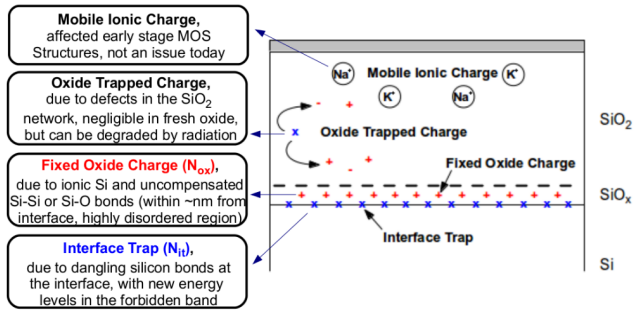

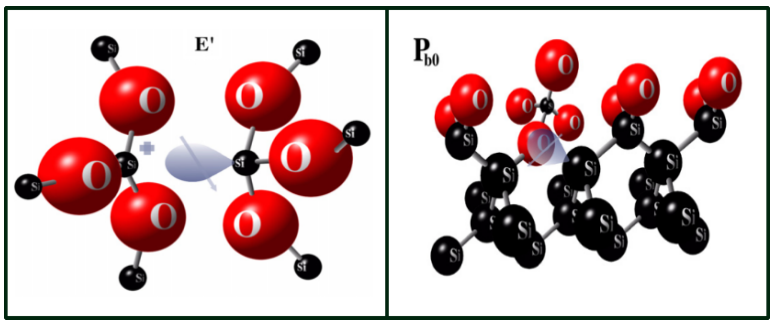

Systematic irradiation tests on the QA procedure

- Irradiation tests performed on test structures (MOS, GCD), miniaturized sensors (Baby sensors)
- X-ray tests on test structures: MOS, GCD
  - Dose up to 40 kGy
  - Investigation that the behavior surface defects are not modified during production

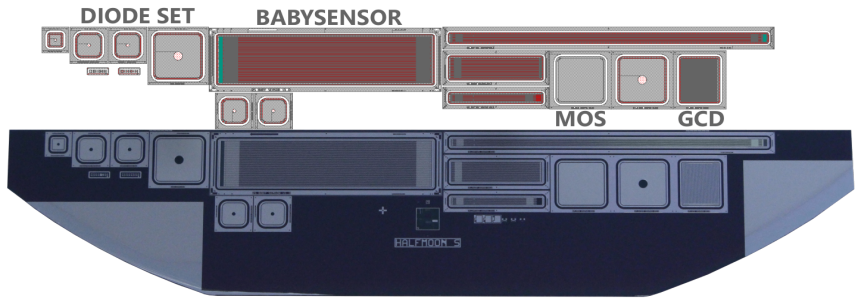

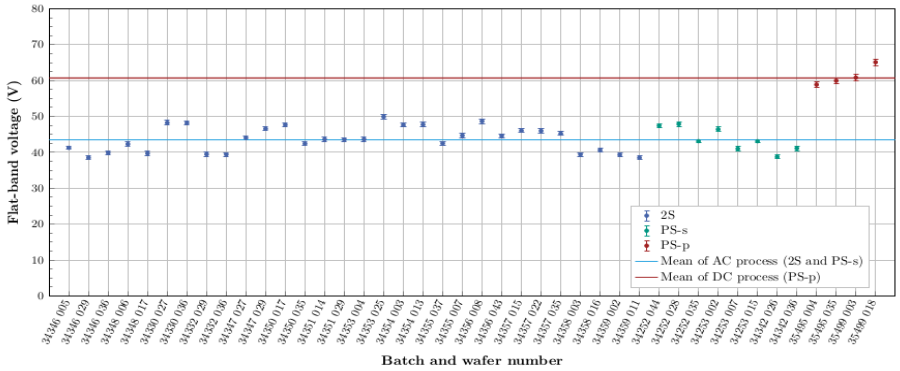

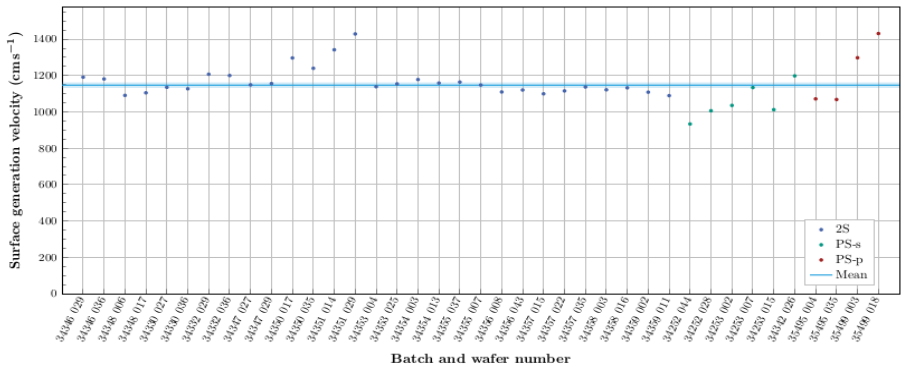

Systematic irradiation tests on the QA procedure

- Iradiation tests with neutrons and protons: Miniaturized strip sensors
- 2S and PS-s sensors irradiated at the maximum expected fluences (p+n)
  - **2S**: $\Phi_{2S} = 3.0 \times 10^{14}$ n_{eq}/cm^2
  - **PS**: $\Phi_{PS} = 1.0 \times 10^{15}$ n_{eq}/cm^2
- Two type of sensors FZ290, thFZ240
  - FZ290: baseline sensor
  - thFZ240: with thinned backside implantation (only $\sim$5 μm in the backside)
- Seed signal measured over annealing time biased at:
  - **600V**: maximum operation voltage after irradiation
  - **800V**: foreseen for regions receiving higher fluences
- For the 2S:, the FZ290 sensors are well in above limit (MPV $>$ 3$\times$threshold $= 12000e^-$, CBC ship)
- For the PS:, the FZ290 well above (MPV $>$ 3$\times$threshold $= 9600e^-$) with a boost at 800V

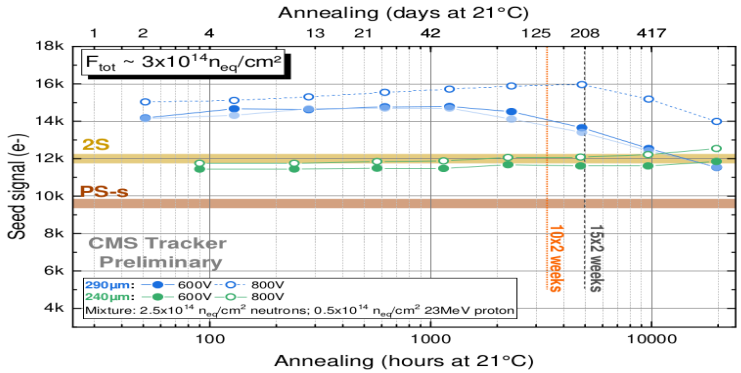

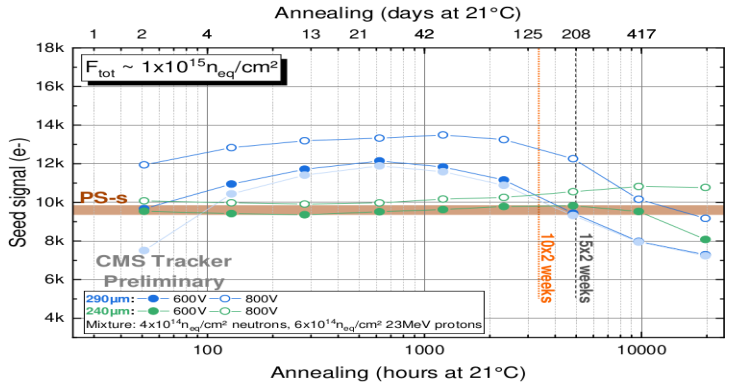

Step	Temperature °C	Time min	Eq. Time at RT days
1	60	**10**	3.8
2	60	20	6.9
3	60	40	13.3
4	60	80	27.9
5	60	100	53.7
6	60	140	100.0
7	80	25	203.1
8	80	57	407.4
9	80	120	824.1

Irradiation studies by using a ^{60}Co source

- Irradiation studies with ^{60}Co-γ photons. A picker therapy unit was used as a source
  - Radioactivity: 9.86 TBq
  - Dose rate: 0.96 kGy/h
- During irradiation, the samples were cooled down to (at 8±0.5 °C) by using a Peltier element with microcontroller for the stabilization of the temperature and power.
- A charged equilibrium box was used for absorbing low energy electrons and photons, made of 2 mm thick Pb with a 0.8 mm layer of Al in the interior.
- Irradiation procedure was split in slots of 10-12 hours of irradiation.
- After every slot of irradiation: Annealing in the climatic test chamber at 60 °C for 10 min
- Between irradiation slots: samples stored in freezer at -28 °C

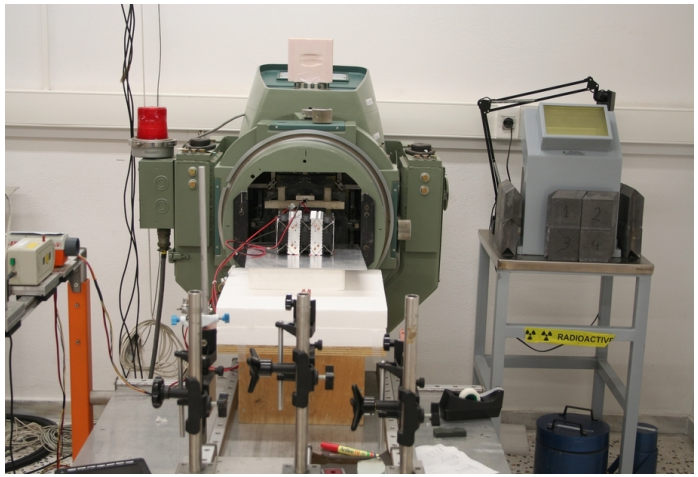

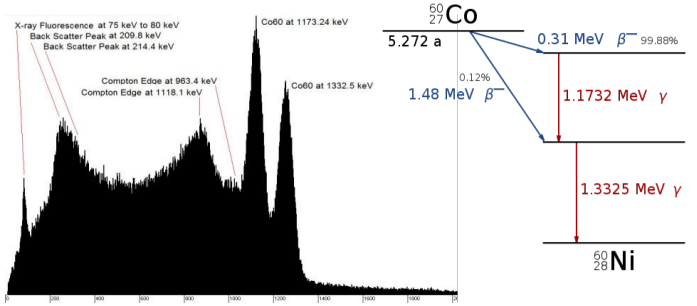

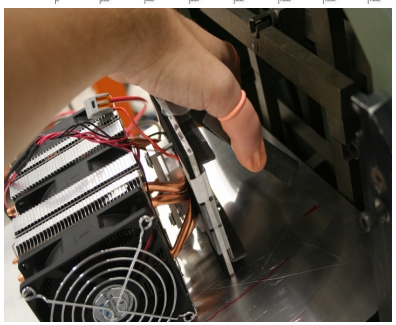

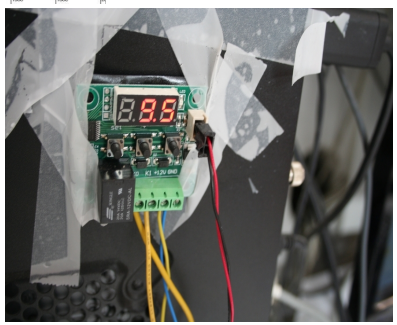

Samples and tests structures

- The samples are built on FZ oxygenated n-in-p wafers. Thinned at 240 μm (physical and active thickness at 240 only ∼5 μm in the backside)
  - Produced for testing purposes as an alternative of the standard FZ290 wafer (physical thickness at 320 μm and active thickness at 290 μm)
- Each test structure contains among others: 1 rectangular MOS capacitor and a gate-controlled diode (GCD) with a metal gate.

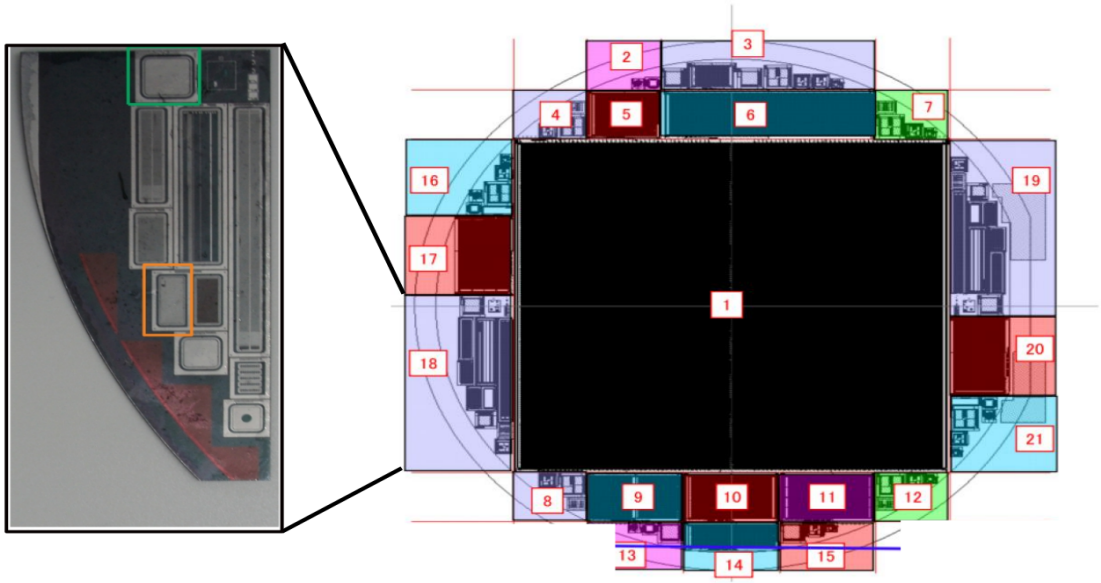

Package Label Name

1 Main Sensor
2 D 1PS 2GR etc (Upper)
3 Sensor PS light etc
4 VDP Flute etc (Upper Left)
5 Sensor No Pstop
6 Sensor Baby
7 VDP Flute etc (Upper Right)
8 VDP Flute etc (Lower Left)
9 Sensor Center Bias Contact
10 Sensor KIT test
11 Sensor Seg Area
12 VDP Flute etc (Lower Right)
13 D 1PS 2GR etc (Lower)
14 Sensor Irradiation
15 MOS & Diode
16 SIMS etc (Left)
17 Sensor PStop Geo
18 HMSet (Left)
19 HMSet (Right)
20 Sensor PCommon
21 SIMS etc (Right)

- Irradiation tests have been performed also for the production wafers (FZ290) with MOS, GCD and FET structures. For more details on this see: https://agenda.infn.it/event/22092/contributions/166554/

Experimental results from the thFZ240 wafers

- The irradiation shifts the flat band voltage of the CV curve to higher values.
- This is a clear evidence of positive charge that is accumulated in the oxide $N_{ox} \propto V_{fb}$.
- Also a small sift in the slope is noticed which due to the increase of interface traps N_{it}.

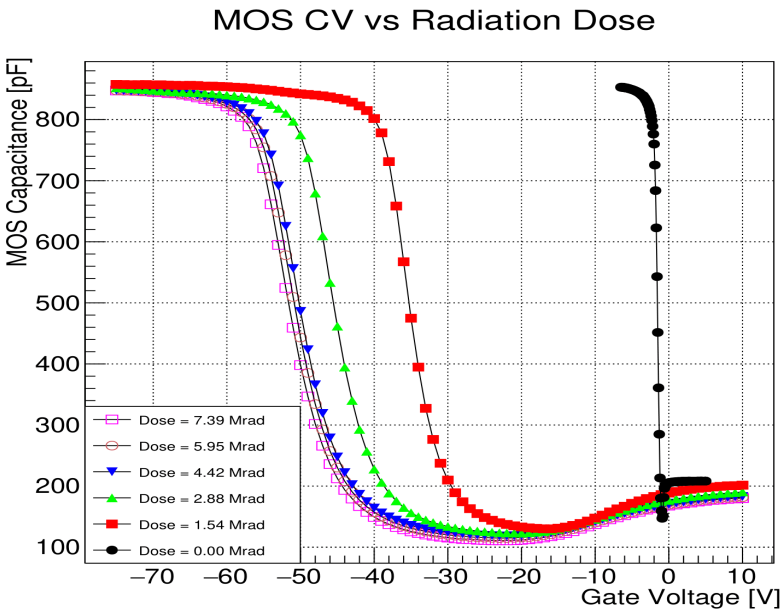

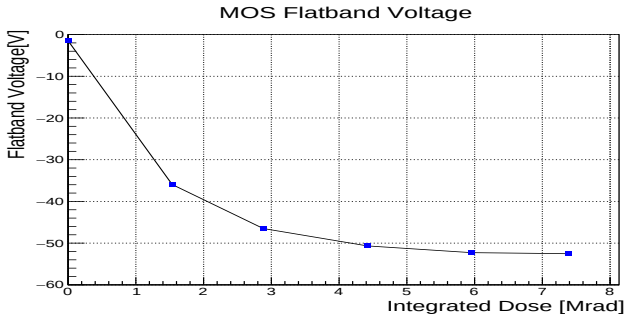

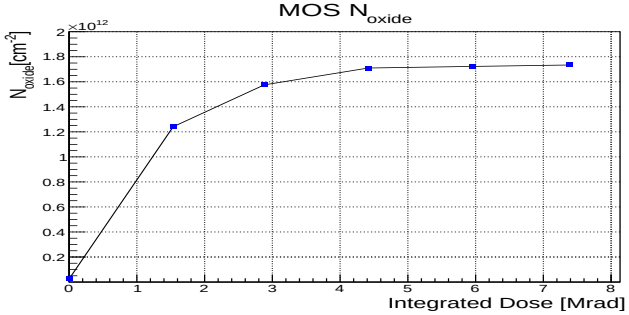

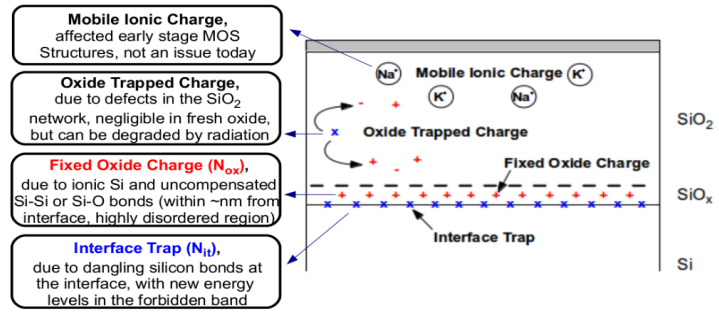

TCAD simulation of MOS capacitor

- TCAD simulations were performed in order to represent the behavior of the MOS capacitor before and after irradiation
- The model that was used is the "New Perugia" model. More details can be found in [2].
  - The model combines the *bulk damage* with the *surface damage* effects.
  - It uses a three level model for the bulk damage effects.
  - It features two uniform trap energy distribution bands, one for donor- and one for acceptor-like defects.
- It has been proven to work well for X-rays up to 10 Mrads and neutron equvalent fluxes up to 10^{15} n_{eq}/cm^2

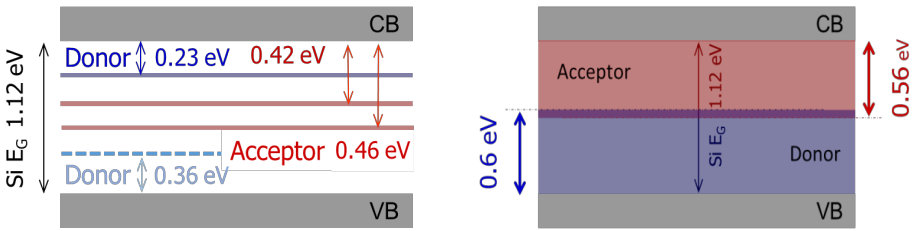

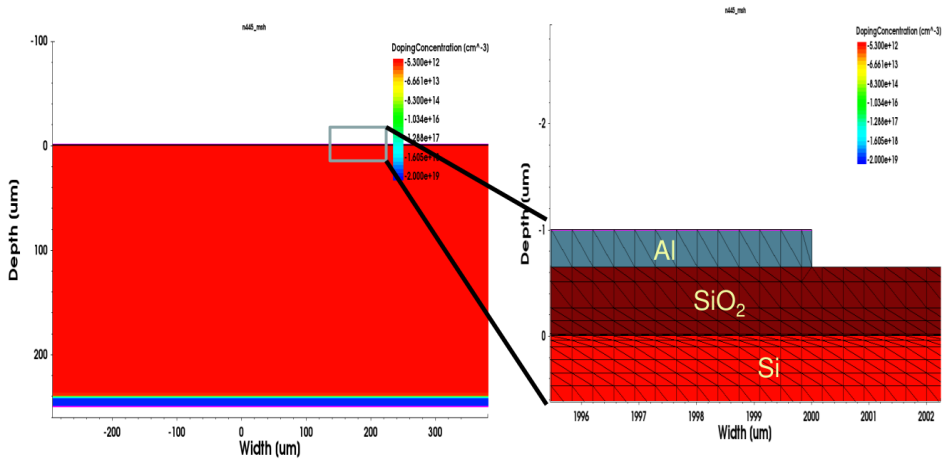

- The model could represent well the unirradiated case

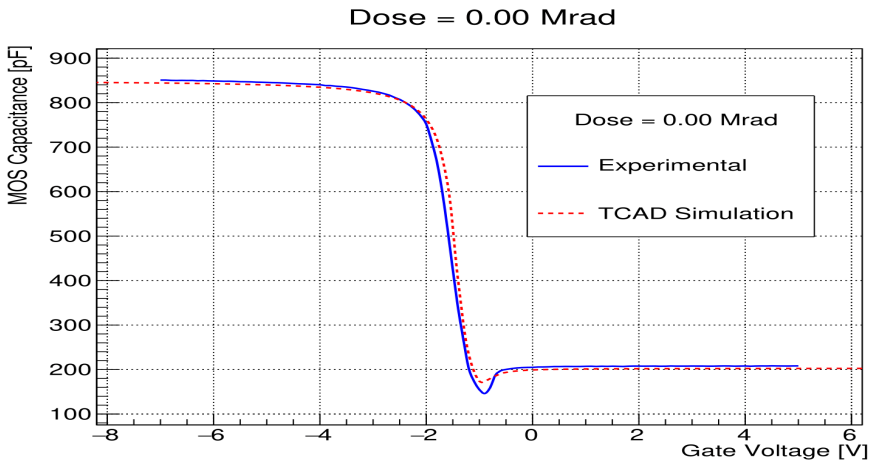

[2] A. Morozzi et al. PoS (Vertex2019) 050,https://doi.org/10.22323/1.373.0050

Modified TCAD Model

- We proposed a modification of the surface parameters of the Perugia model that can represent better the irradiation results from a ^{60}Co source.
- Both the oxide charge density and interface trap state density are modeled as the sum of the value before irradiation and the radiation induced increase

Type	Energy (eV)	Band width (eV)	σ_e (cm^2)	σ_h (cm^2)
Donor	$E_V < E_T < E_V + 0.54$	0.54	1.0×10^{-15}	1.0×10^{-16}
Acceptor	$E_C - 0.58 < E_T < E_c$	0.58	1.0×10^{-16}	1.0×10^{-15}

$$\Delta Q_{ox}(x) = Q_{ox}(0) + \Delta Q_{ox}(x)$$

$$\Delta N_{IT_{acc}}(x) = N_{IT_{acc}}(0) + \Delta N_{IT_{acc}}(x)$$

$$\Delta N_{IT_{don}}(x) = N_{IT_{don}}(0) + \Delta N_{IT_{don}}(x)$$

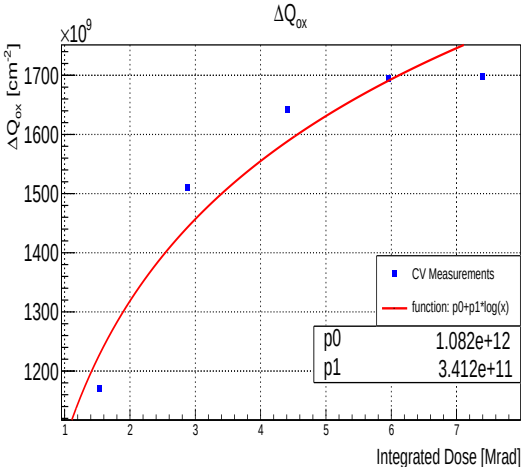

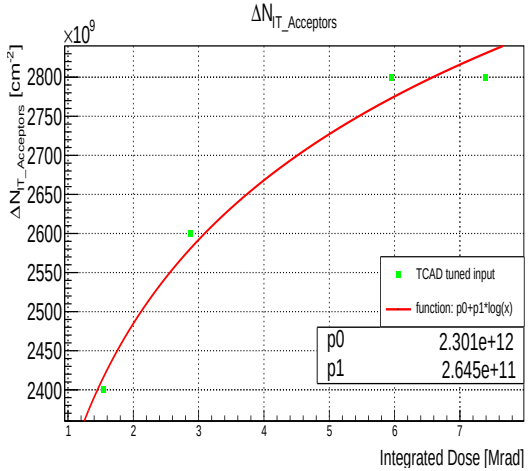

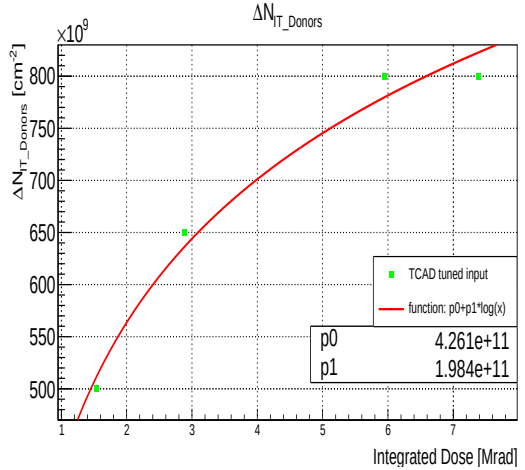

- Parametrization of the shifts of Q_{ox} and interface traps

$$\Delta Q_{ox}(x) = 1.08 \cdot 10^{12} + 3.41 \cdot 10^{11} ln(x) \quad [\text{cm}^{-2}]$$

$$\Delta N_{IT_{acc}}(x) = 2.30 \cdot 10^{12} + 2.65 \cdot 10^{11} ln(x) \quad [\text{cm}^{-2}]$$

$$\Delta N_{IT_{don}}(x) = 4.26 \cdot 10^{11} + 1.98 \cdot 10^{11} ln(x) \quad [\text{cm}^{-2}]$$

- where x is the radiation dose in Mrad

^{60}Co Irradiated MOS and TCAD model

- The proposed modifications work reasonably well for ^{60}Co γ photons with doses up to 74kGy = 7.4Mrad

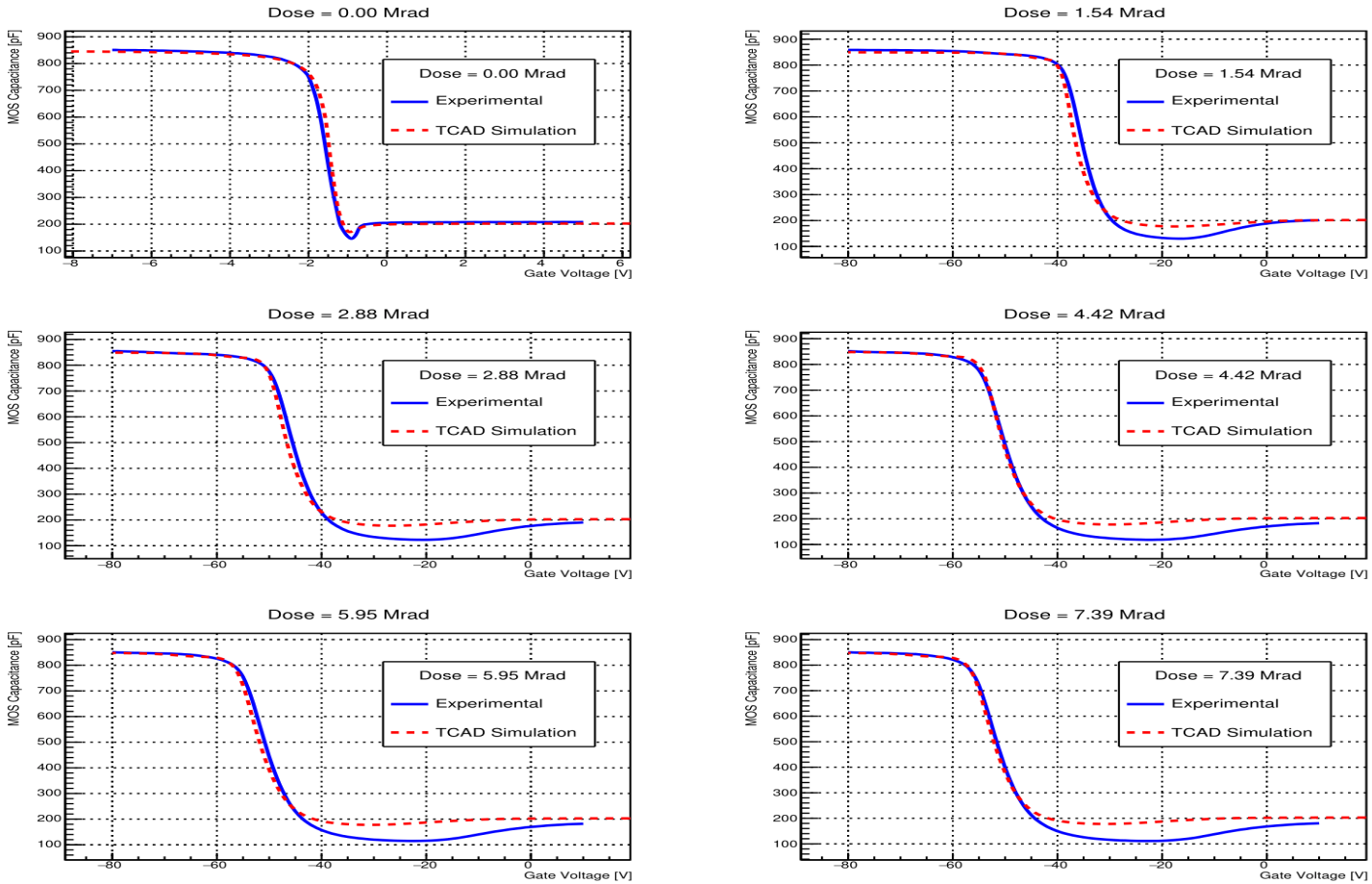

[3] P. Asenov, P. Assiouras, A. Boziari, K. Filippou, I. Kazas, A. Kyriakis, D. Loukas, A. Morozzi, F. Moscatellid and D. Passerid, Study of p-type silicon MOS capacitors at HL-LHC radiation levels through irradiation with a cobalt-60 gamma source and a TCAD simulation," JINST **16** (2021) no.06, P06040

Summary on Irradiation tests by using a ^{60}Co source

- In this work silicon MOS capacitors were irradiated with ^{60}Co photons.
- The level of the radiation-induced charge in the test structures was determined from the shift of the flat band voltage in the MOS capacitors after irradiation and a saturation effect was observed.
- In addition significant change in the slope of the depletion region was observed which is related to the interface charge concentration.
- The measurements were compared with the results of a TCAD simulation based on a modified version of the ”New Perugia model”, which takes into account several radiation damage effects.
- The modified model describes reasonably well our experimental measurements from ^{60}Co γ photons and could be seen as a complementary model to the “New Perugia model” that describes well the X-ray irradiation and the irradiation with charge and neutral particles.

Publications and conferences related to this work

- **Publications**:
  - Patrick Asenov, Panagiotis Assiouras, Argiro Boziari, Konstantinos Filippou, Ioannis Kazas, Aristotelis Kyriakis, Dimitrios Loukas, Arianna Morozzi, Francesco Moscatellid, and Daniele Passerid. **Study of p-type silicon MOS capacitors at HL-LHC radiation levels through cobalt-60 gamma source and TCAD simulation**. 3 2021.
  - P. Assiouras, P. Asenov, A. Kyriakis, and D. Loukas. **Fast calculation of capacitances in silicon sensors with 3D and 2D numerical solutions of the Laplace's equation and comparison with experimental data and TCAD simulations**. JINST, 15(11):P11034, 2020.
  - W. Adam et al. **Characterisation of irradiated thin silicon sensors for the CMS phase II pixel upgrade.** Eur. Phys. J., C77(8):567, 2017.
  - W. Adam et al. **P-Type Silicon Strip Sensors for the new CMS Tracker at HL-LHC.** JINST, 12(06):P06018, 2017
- **Conferences**:
  - **Study of p-type silicon GCD and FET structures irradiated with a Cobalt-60 gamma source at HL-LHC radiation levels and TCAD simulations.** P.Assiouras on behalf the CMS collaboration, 15th Pisa Meeting on Advanced Detectors, La Biodola - Isola d'Elba (Italy), May 24-28, 2022.
  - **Process quality control of silicon sensors for the Phase-2 upgrade of the CMS Outer Tracker for the HL-LHC.** P.Assiouras on behalf the CMS collaboration, 17th (Virtual) Trento Workshop on Advanced Silicon Radiation Detectors, University of Freiburg, Mar 2-4, 2022.
  - **Process quality control of silicon sensors for the Phase-2 upgrade of the CMS Outer Tracker.** P.Assiouras , HEP 2021, Thessaloniki, Greece Recent Developments in High Energy Physics and Cosmology, Annual meeting of the Hellenic Society for the Study of High Energy Physics.
  - **Fast calculation of capacitances for silicon detectors with a 3D and2D numerical solution of the Laplace's equation. Comparison withexperimental results and TCAD simulations.**, Vertex 2019, The 28th International Workshop on Vertex Detectors, 13-18 October 2019, Croatia
  - **A method for fast calculations of capacitances in micro-strip and micro-pixel detectors in High Energy Physics.** P.Assiouras , HEP 2017, Ioannina, Greece, Recent Developments in High Energy Physics and Cosmology, Annual meeting of the Hellenic Society for the Study of High Energy Physics.

Thank you very much for your attention!!!

Backup slides

Phase-2 extras

Tilted Barrel Geometry

- Stubs generation works only if the charged particle cross the two sensors on the same halve of the same module
  - This is not true for (flat) barrel peripherical modules.
- The Phase-2 CMS TRacker will use (increasingly) tilted peripherical barrel modules.
  - Stub finding efficiency increase with tilted geometry at the barrel edges.
  - In addition, the number of modules needed is decreased. From ∼15k (flat geometry) to ∼13k (tilted geometry). Decreasing also the material budget

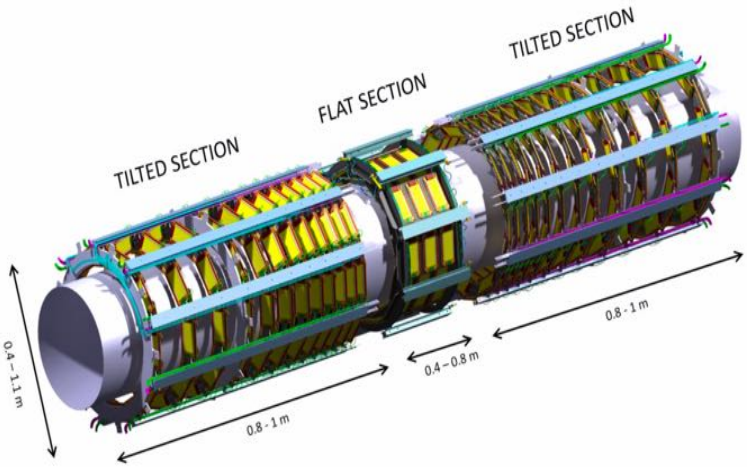

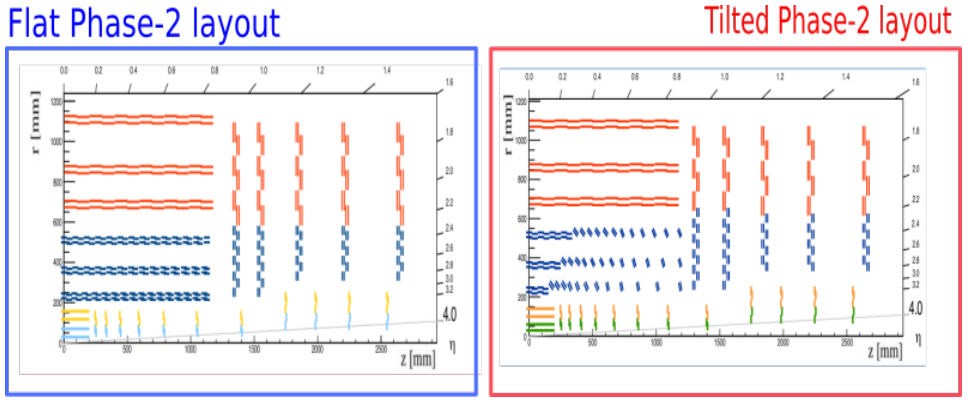

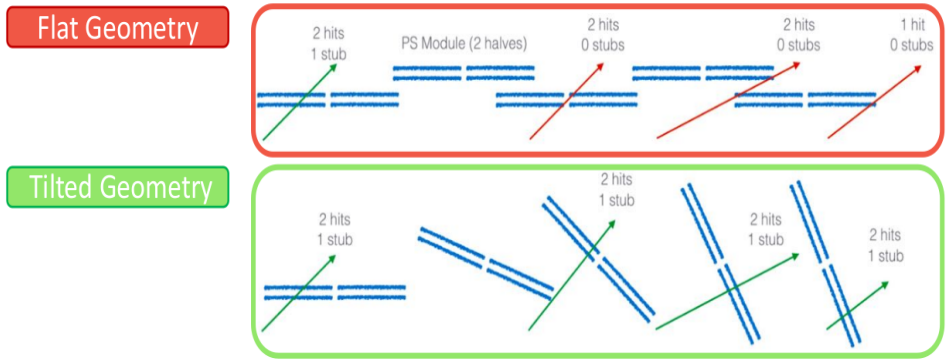

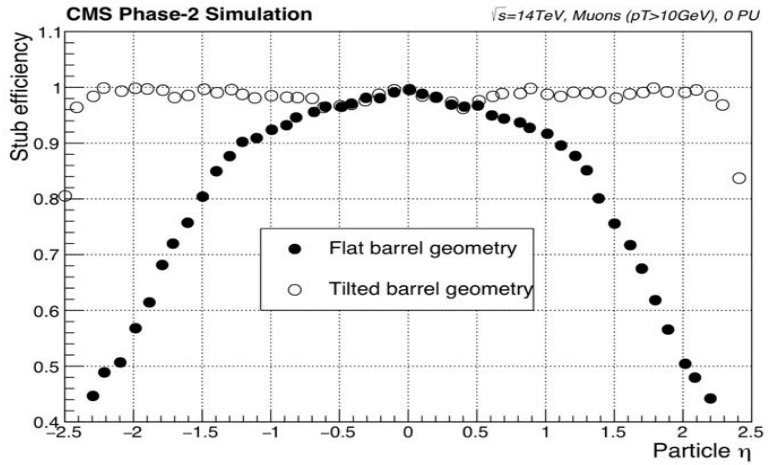

Radiation-hard sensors

- Extensive R&D campaign started on 2010 to investigate different material options, thicknesses, and manufacturers. The outcome was:
  - Materials: Planar float zone n-in-p silicon sensors are best suited for the Phase-2 Outer Tracker (than the p-in-n silicon sensors of the current Tracker).
    - Better behavior after irradiation
  - Manufacturer: CMS chose Hamamatsu as the most suitable vendor for the Outer Tracker upgrade.
  - Thinning process: Standard material (FZ290) with 320μm physical (290μm active) thickness chosen as the best option (same process as in the current Tracker).
    - Other options: Thinned material with physical thickness ≈ active thickness (thFZ240),followed by polishing and deep diffusion material, by expanding the implantation in the backside (ddFZ240).
    - Irradiation tests reaching the max 2S fluence after 3000 fb^{-1} (ultimate scenario) the thFZ240 sensors barely reaches 2S limit, while FZ290 is well above
    - Further considerations about handling (thinned sensors are more prone to scratch-induced early IV breakdowns), and costs led to the choice of FZ290 sensors

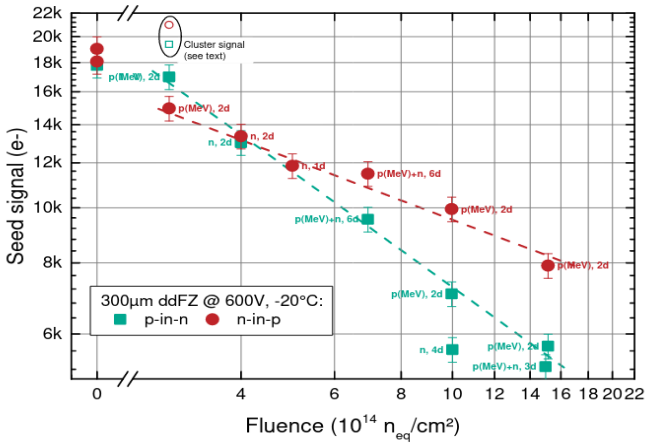

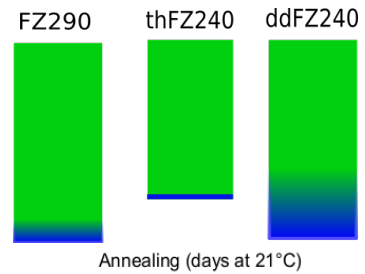

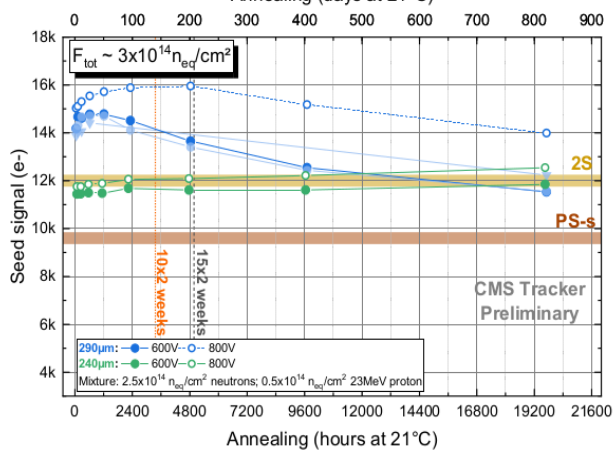

Silicon sensor general

Silicon strip and pixel detectors

- Highly segmented silicon detectors have been used in Particle Physics experiments for nearly 30 years.
- Two commonly used detectors in High Energy Physics experiments are :
  - Micro-strip detectors
    - One surface is segmented in one axis to form strips with regions of p+ (or n+ doping).
    - Forming a 1D matrix of n+p diodes.
    - The trajectory of an incident particle is projected on the strips
    - Detects the passage of ionizing radiation with high spatial resolution, good efficiency and relatively low cost.
  - Hybrid pixel detectors
    - Segmented in two axis to form pixels of p+ (or n+ doping)
    - Forming a 2D matrix of n+p diodes.
    - Connection by “bump bonding”.
    - Every cell is connected to each own processing electronics.
    - Requires more sophisticated readout architecture
    - More robust in radiation damage. Usually placed in the innermost parts of HEP experiments

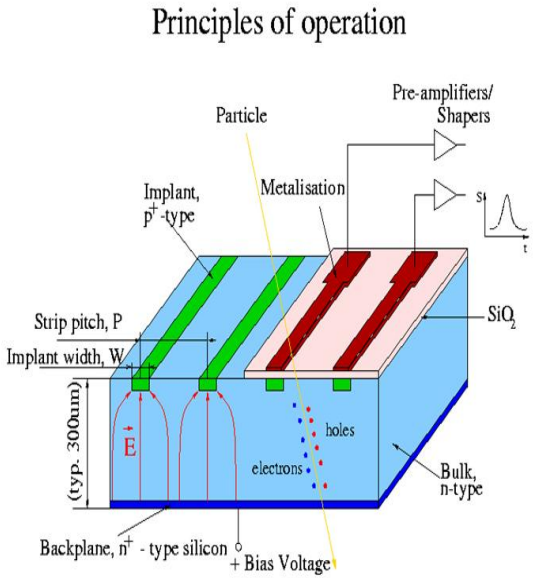

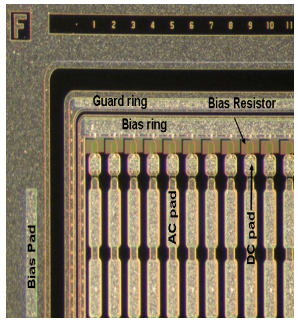

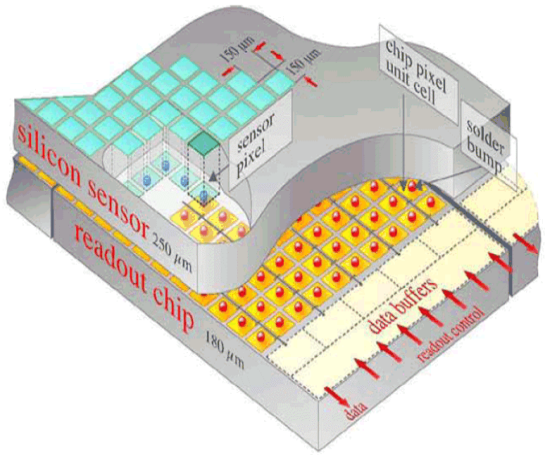

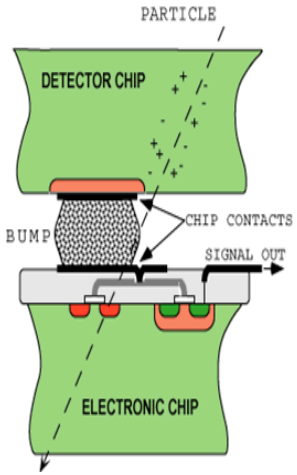

Planar silicon strip sensors-Fabrication procedure

Outer Tracker will encompass 200 m^2
Consisting of 24000 sensors
Two different modules with three different sensors

- 2S sensors: $6''$ wafers, FZ n-on-p, Act. thick. 290 um, AC coupled
- PS-s sensors: $6''$ wafers, FZ n-on-p, Act. thick. 290 um, AC coupled
- PS-p sensors: $6''$ wafers, FZ n-on-p, Act. thick. 290 um, DC coupled

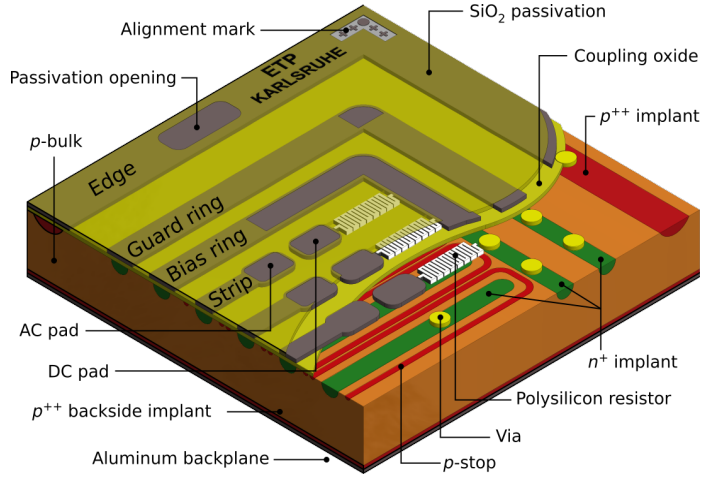

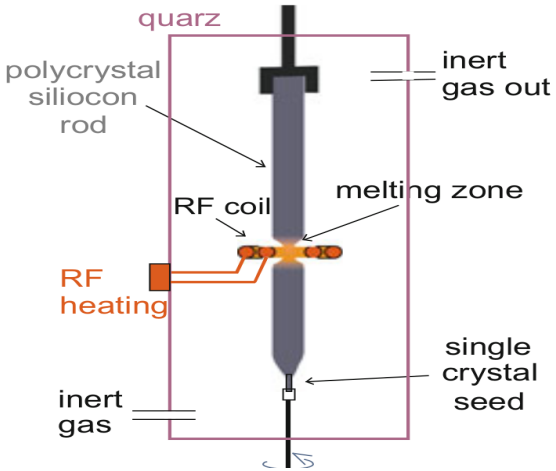

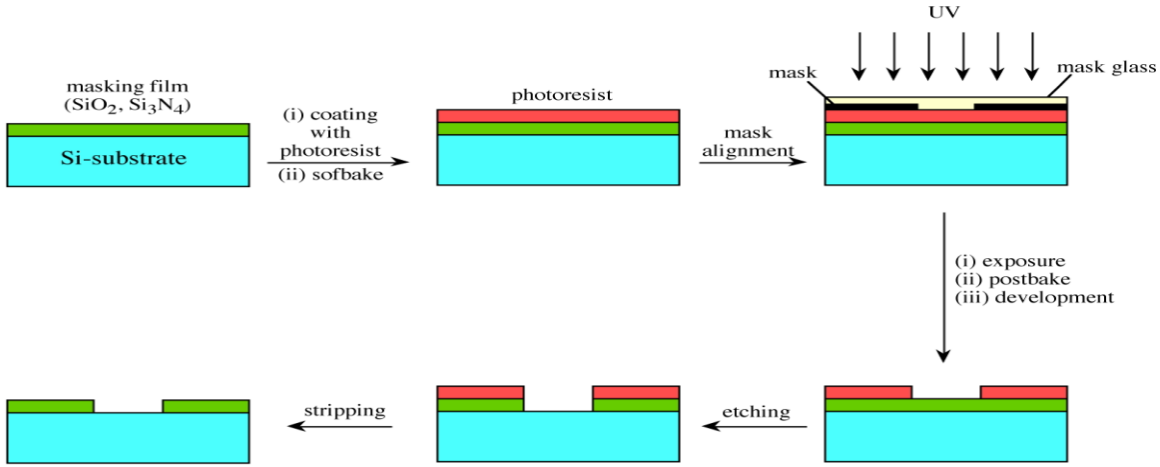

Polysilicon and punch-through biasing / AC and DC coupled sensors

- AC coupled sensors:
  - Coupling capacitor is integrated in the sensor. (SiO_2)
  - Blocks leakage current from the sensor and the DC component of the signal
  - Needs polysilicon resistors for the biasing which are connected to implantation.

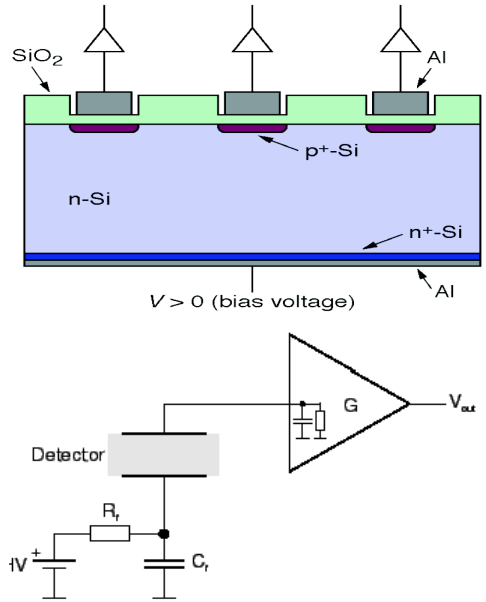

- DC coupled sensors:
  - Coupling capacitor is integrated in the read-out chip. (SiO_2)

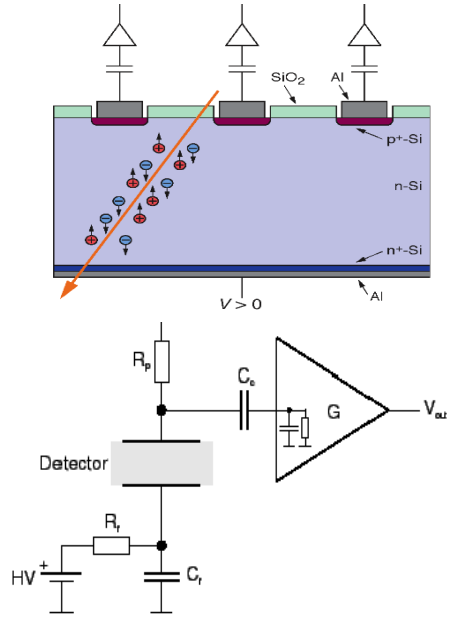

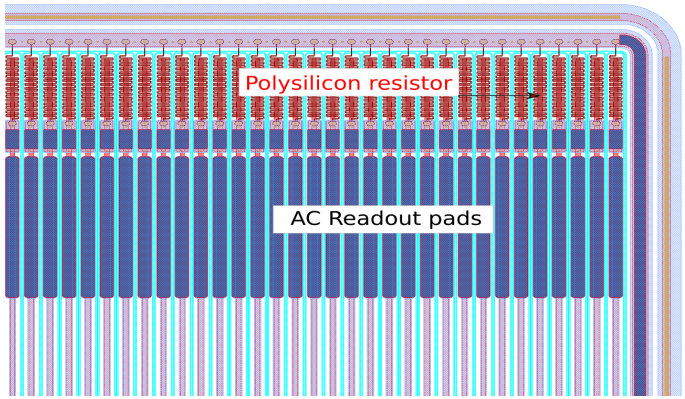

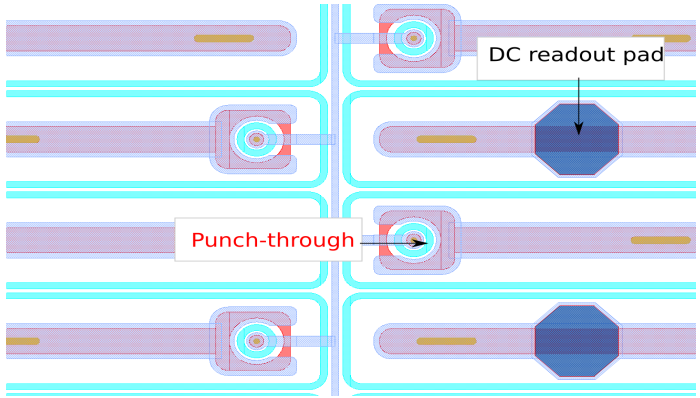

Quality control extras

Sheet resistance - VDP measurements

- The resistance of a conductor material is given by:

$$R = \rho \frac{L}{A} = \frac{\rho}{t} \frac{L}{W} = R_{sh} \frac{L}{W} [\Omega] \qquad (4)$$

where L is the length and $A = Wt$ the cross section surface

- The sample can be subdivided into squares of width W, $L/W = N_{squares} (\approx 3000)$
- Van der Pauw proved that the expression below holds for a semi-infinite plane and also for an arbitrary shape

$$e^{-\pi \frac{t+R_{DA,BC}}{\rho}} + e^{-\pi \frac{t+R_{DC,AB}}{\rho}} = 1 \qquad (5)$$

- For $t \to 0$ and a symmetrical structure $(R_{DA,BC} = R_{DC,AB} = R)$

$$R_{sh} = \rho/t = \frac{\pi}{ln(2)} R \qquad (6)$$

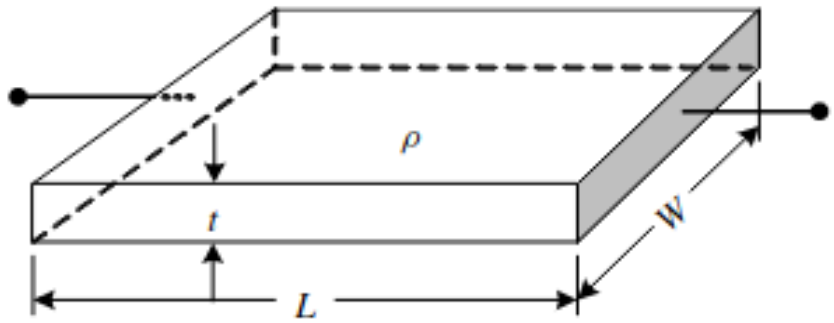

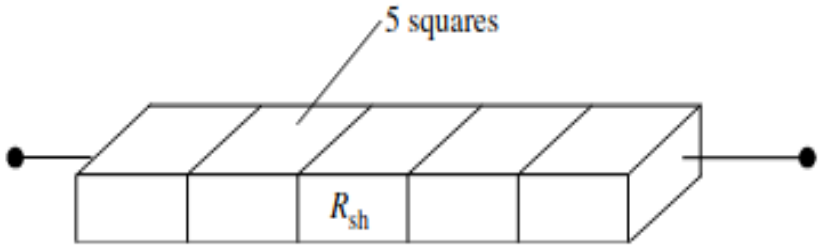

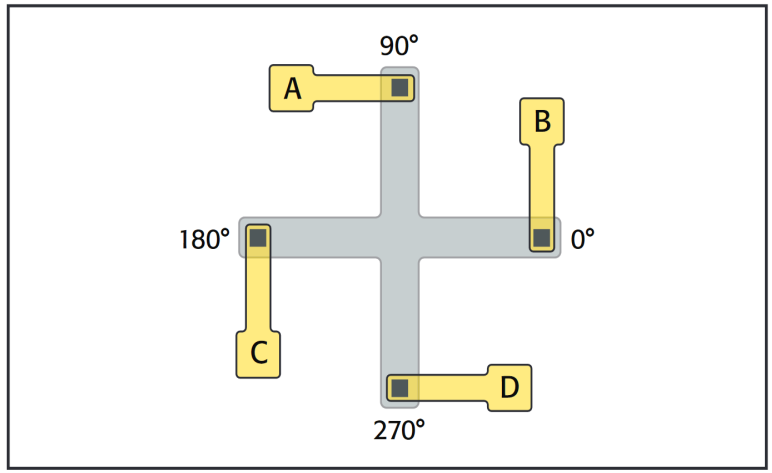

GCD working principle

- A small bias is applied to the diode → Small depletion region formed around the junction
- The gate voltage is then varied:
  - Accumulation ($V_{gate} \ll V_{fb}$): Only the diode current is measured I_{jd}, majority carriers accumulate beneath the oxide
  - As the voltage increase the area beneath the gate deplete and connects with the depletion area of the diode
  - Depletion ($V_{gate} > V_{fb} + V_{diode}$): The electric field drives the surface current I_{ox} which is produced from the interface traps towards the diode
  - Inversion ($V_{gate} > V_{fb}$): Electrons are accumulated beneath the oxide that stops the flow of current from the interface. $I_{gd} + I_{jd}$
- Non-ideality in the PQC measurmets: Lateral extension of the depletion area beneath the oxide
  - Non negligible thermal generation can occur due to unscreened interface states

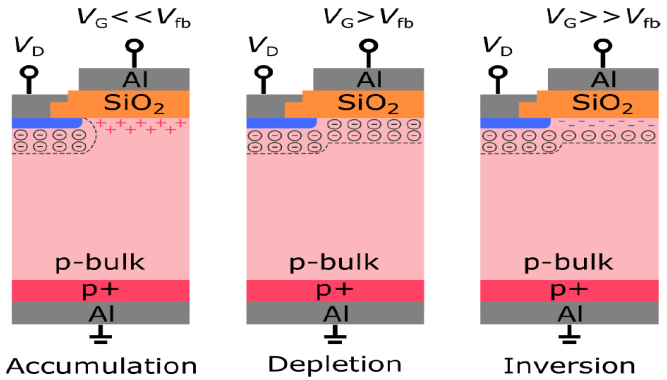

$$I = I_{ox} + I_{jd} + I_{gd} \tag{7}$$

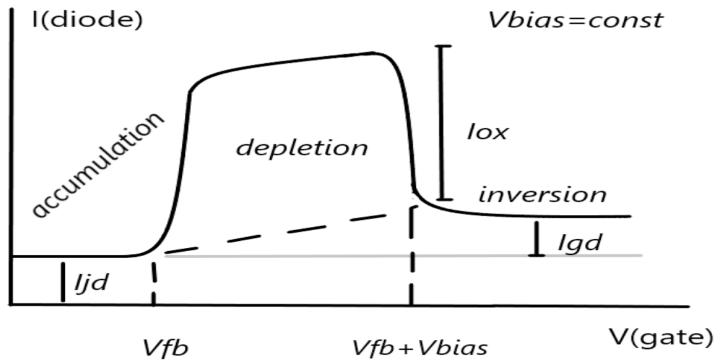

G. Verzellesi, et all, "On the accuracy of generation lifetime measurement in high-resistivity silicon using PN gated diodes," 817-820, April 1999, doi: 10.1109/16.753724.

MOS working principle

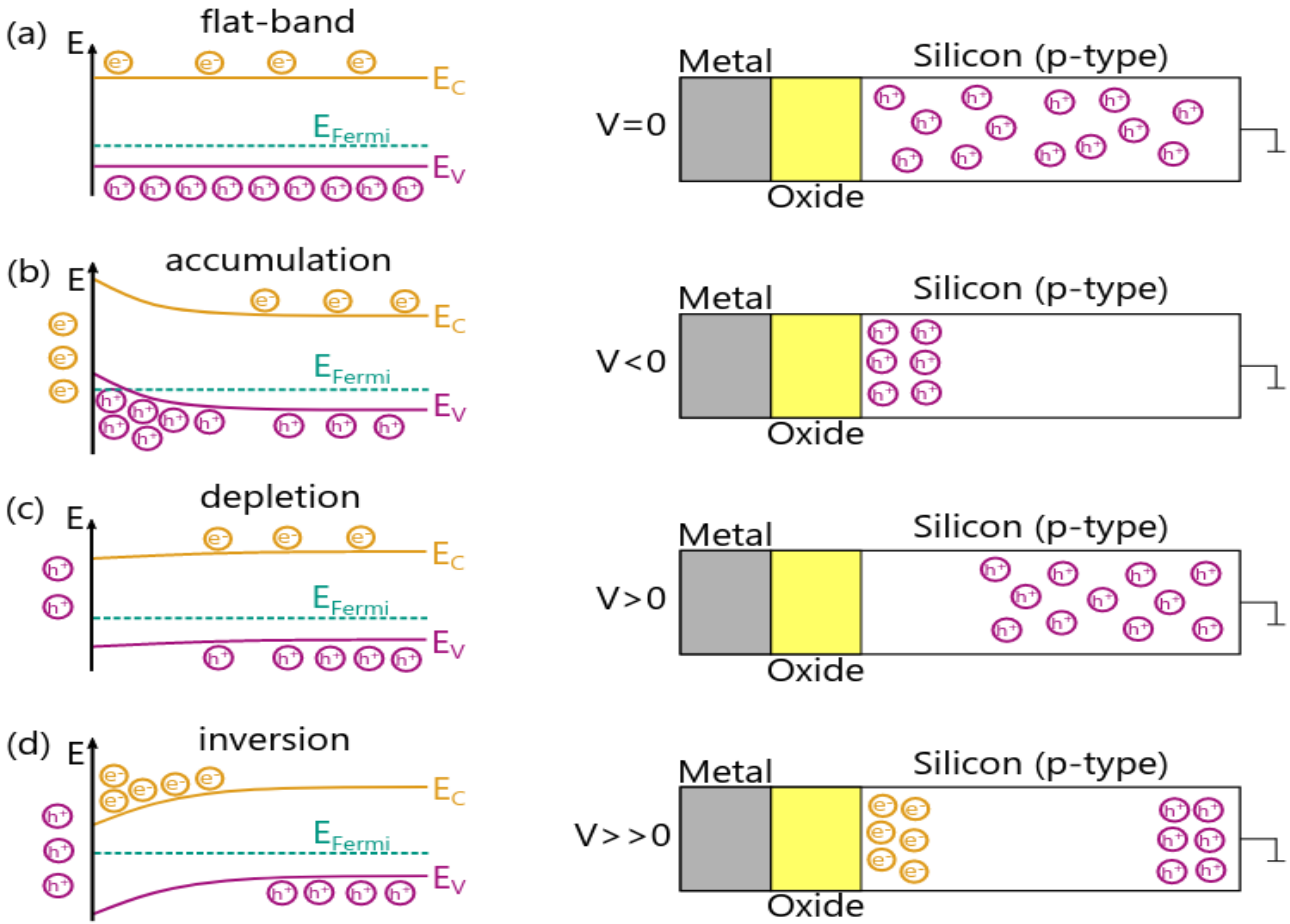

Diodes

- Diodes are used in order to study of the bulk properties. The standard type of measurements are IV and CV measurments:

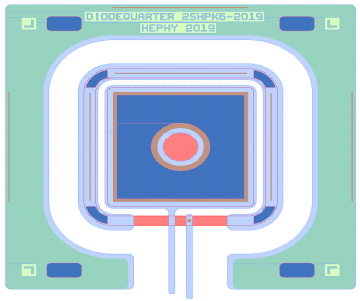

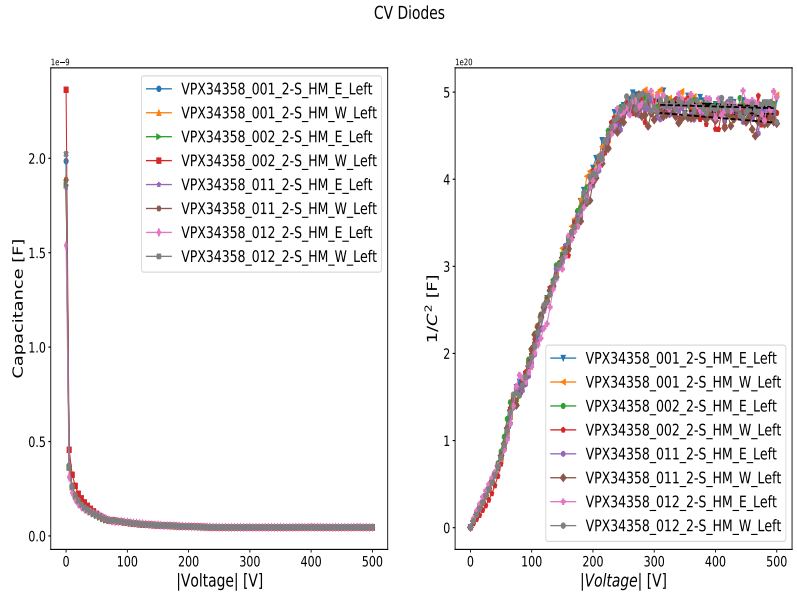

- CV Measurments:
  - Full depletion Voltage V_{fd}
  - Doping concentration N_{sub}
  - Bulk resistivity $\rho > 2.7\ k\Omega cm$

$$\rho = \frac{d^2}{2\epsilon_0 \epsilon_{Si} \mu_h V_{fd}}$$

- IV Measurments:
  - Current value at 600V ($< 2.5\ nA/mm^3$)
  - Check for breadown voltage

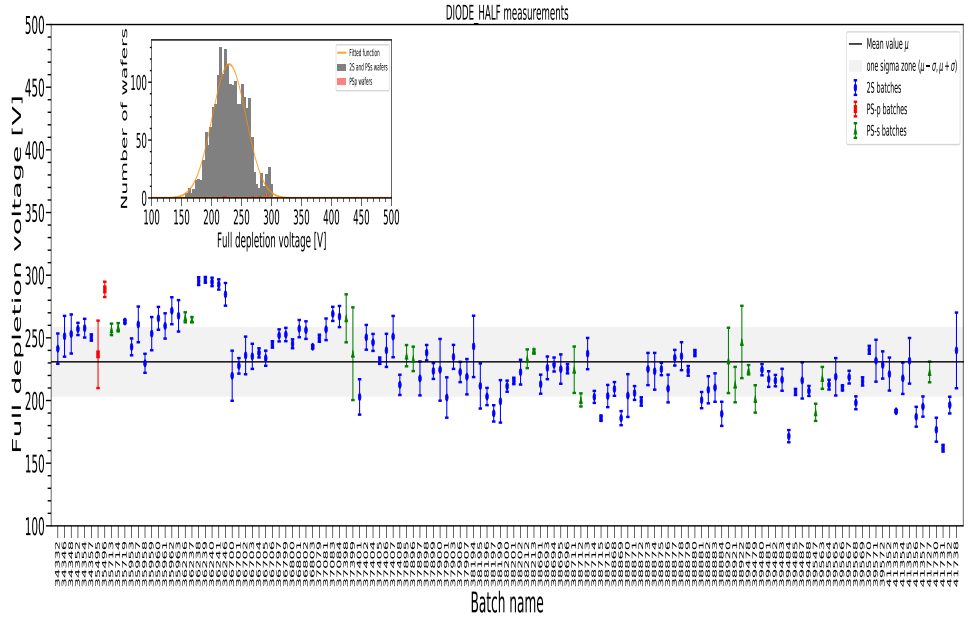

Four point bulk resistivity measurement

- PQC3 flute contains a bulk resistivity cross, for measuring the bulk resistivity.

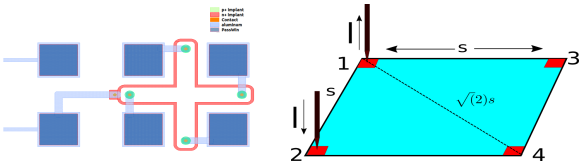

- For a square like structure in a sample with infinite thickness and surface. The bulk resistivity is given by:

$$\rho_\infty = \frac{2\pi s}{2-\sqrt{2}} \frac{V_{34}}{I_{21}} \tag{8}$$

- where s is the pad spacing.For real wafers where $(t \approx s)$. A correction factor is introduced.

$$\rho = F\rho_\infty \tag{9}$$

- By performing the image method for a square like structure for a conducting bottom surface. The correction factor is:

$$F = \frac{1}{1 + \frac{4}{2-\sqrt{2}} \sum_{n=1}^{+\infty} (-1)^n \left[\frac{1}{\sqrt{1+(\frac{2nt}{s})^2}} - \frac{1}{\sqrt{2+(\frac{2nt}{s})^2}} \right]} \tag{10}$$

where t is the wafer thickness.
For $t = 290\ \mu m$ and $s = 187\ \mu m$, $F = 1.089$

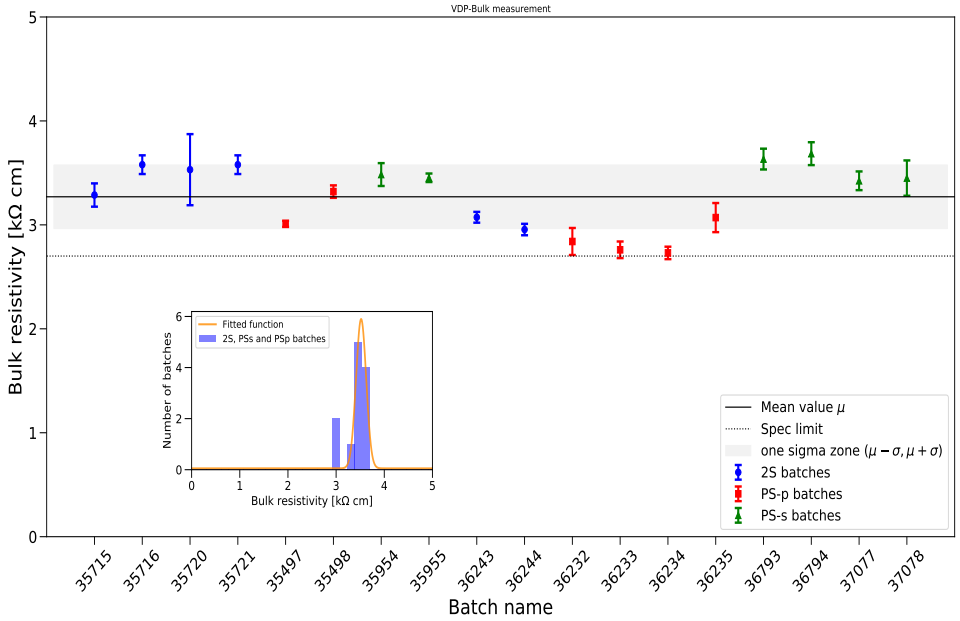

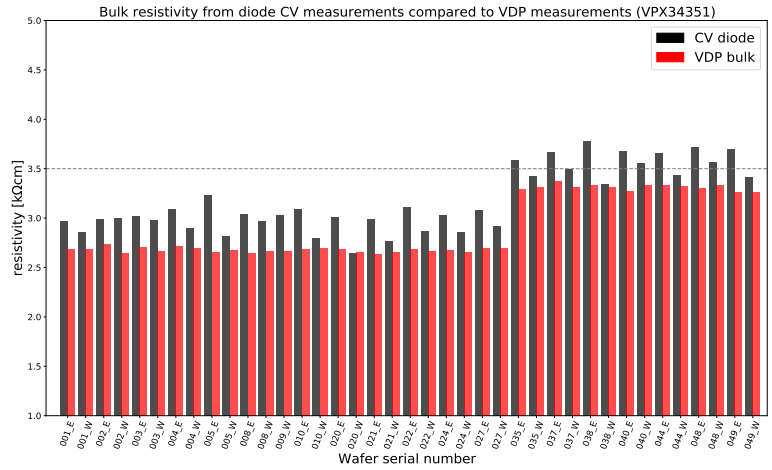

Bulk resistivity: Extraction of the correction factor

- In the case where s<<t:

$$V_3 = \frac{\rho I}{2\pi}\left(\frac{1}{\sqrt{2}s} - \frac{1}{s}\right)$$
$$V_4 = \frac{\rho I}{2\pi}\left(\frac{1}{\sqrt{2}s} - \frac{1}{s}\right)$$

$$V_{34} = \frac{\rho I}{2\pi s}\left(2 - \sqrt{2}\right)$$

$$\rho_\infty = \frac{2\pi s}{2-\sqrt{2}}\frac{V}{I}$$

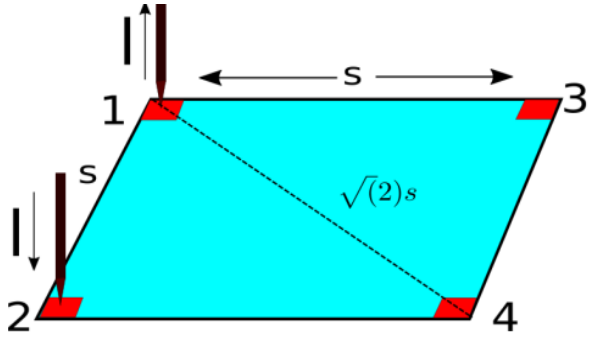

- In the case where s~t: By using image method. For n reflections:

$$V_{tot} = V_0 + V_1 + V_2 + ...V_n$$
$$= \frac{\rho I}{2\pi s}\left(2-\sqrt{2}\right) + \sum_{n=0}^{+\infty}(-1)^n \frac{2\rho I}{\pi s}\left(\frac{1}{\sqrt{((\frac{2nt}{s})^2+1)}} - \frac{1}{\sqrt{((\frac{2nt}{s})^2+2)}}\right)$$

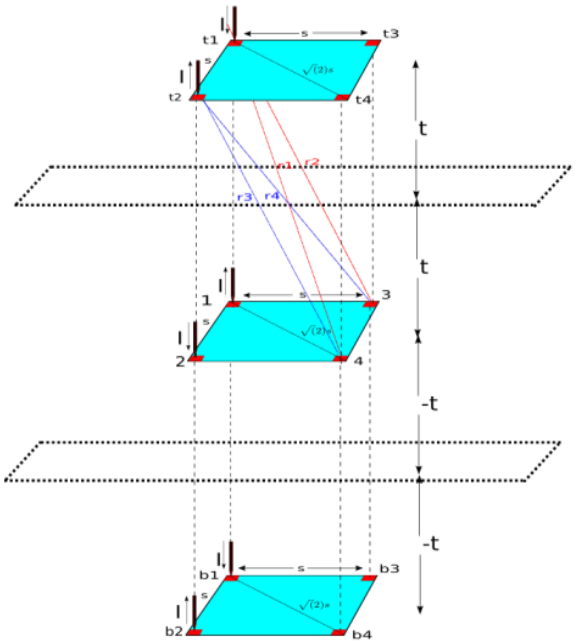

- Then for resistivity: $\rho = \rho_\infty F$

$$F = \frac{1}{1+\frac{4\cdot(-1)^n}{2-\sqrt{2}}\sum_{n=1}^{\infty}\left[\frac{1}{\sqrt{1+\left(\frac{2nt}{s}\right)^2}} - \frac{1}{\sqrt{2+\left(\frac{2nt}{s}\right)^2}}\right]}.$$

For s=187 [μm] and t=290 [μm]: F=1.089

Irradiation tests extras

MOS capacitors

- Electrical measurements:
  - Oscillation amplitude = 250 mV
  - Frequency = 10 kHz
  - Flatband voltage calculated with the first derivative method
- Shift od the flatland voltage to more negative values
- Saturation of the flat-band voltage at -30 V after $\sim$ 40 kGy

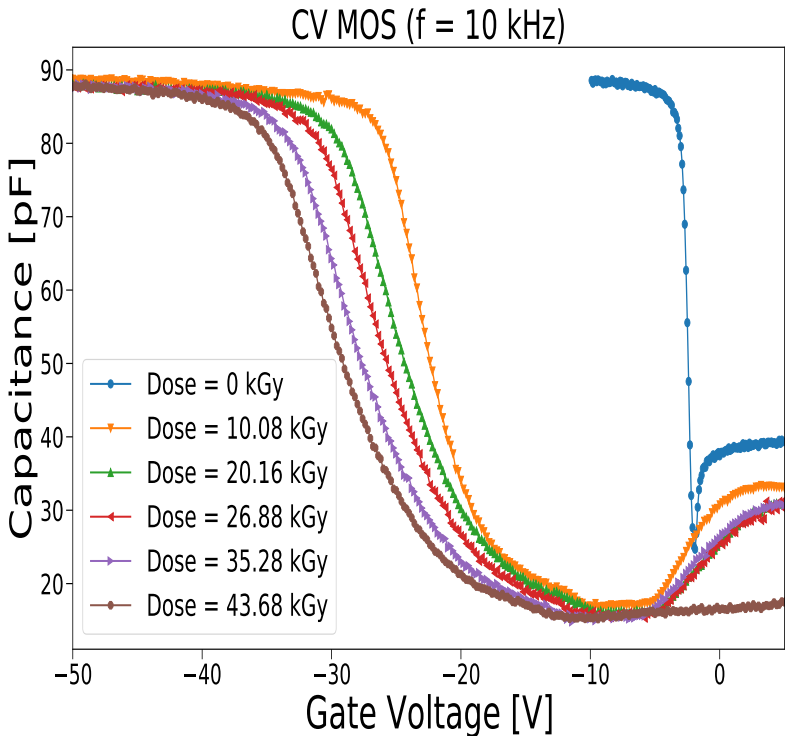

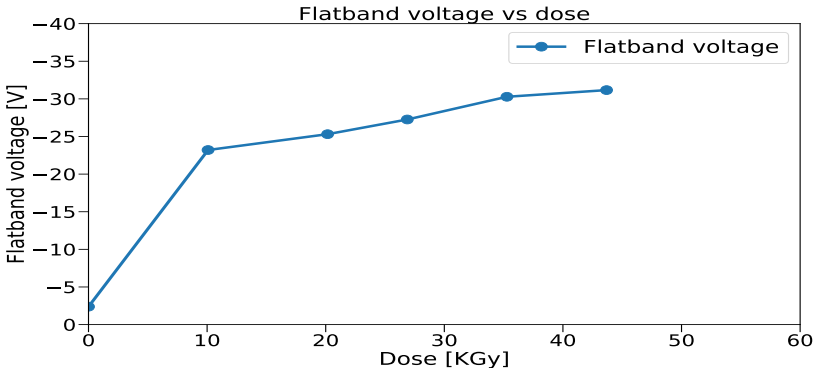

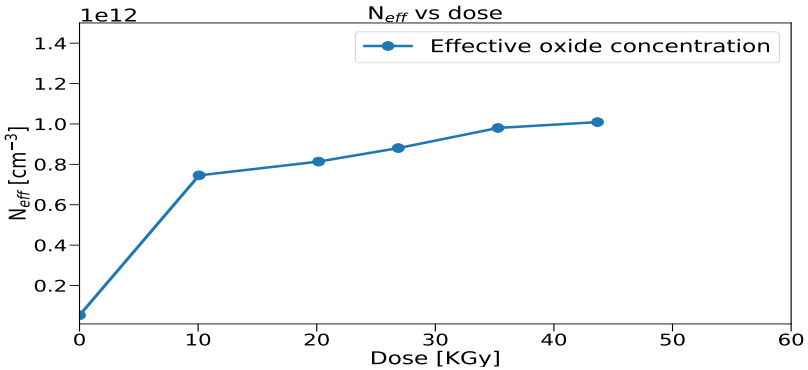

Gated control diodes

- Electrical measurements:
  - Diode voltage on GCD: increased (from +5 to +10 V) for higher doses
  - Current scaled to 20 °C, according to [1]
- Increase of the surface current velocity at 800 cm/ sec after $\sim$ 40 kGy.

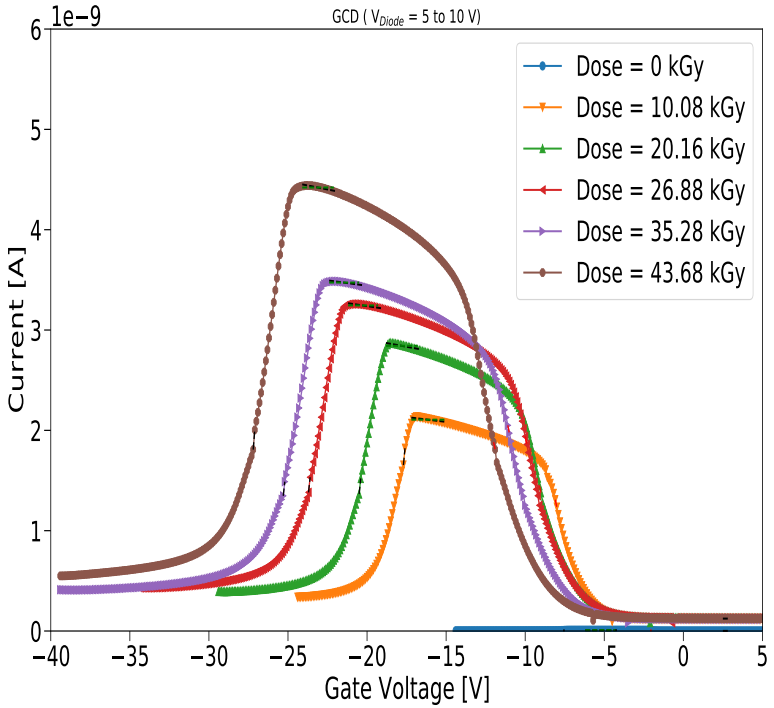

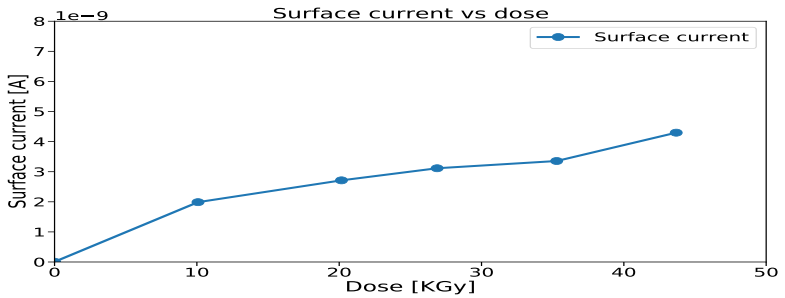

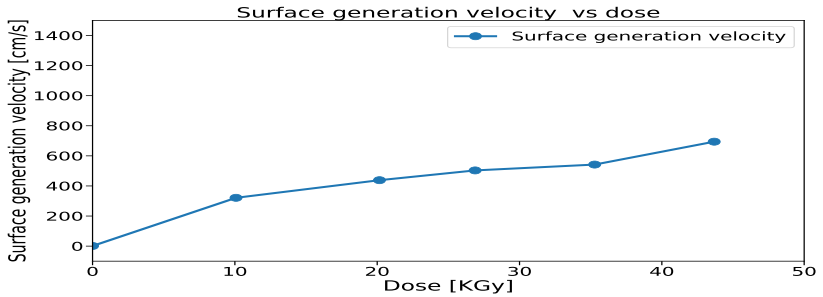

[1] A Chilingarov 2013 JINST 8 P10003 DOI 10.1088/1748-0221/8/10/P10003 .

FET structures

- Electrical measurements:
  - Drain-Source Voltage stable (V_{DS}=100 mV)
  - Threshold Voltage calculated with the ELR method
- Negative shift to the threshold voltage and degradation of the maximum transconductance
- Increase of the threshold voltage after 40 kGy, built up of negative interface trapped charges which compensate the decrease [2]

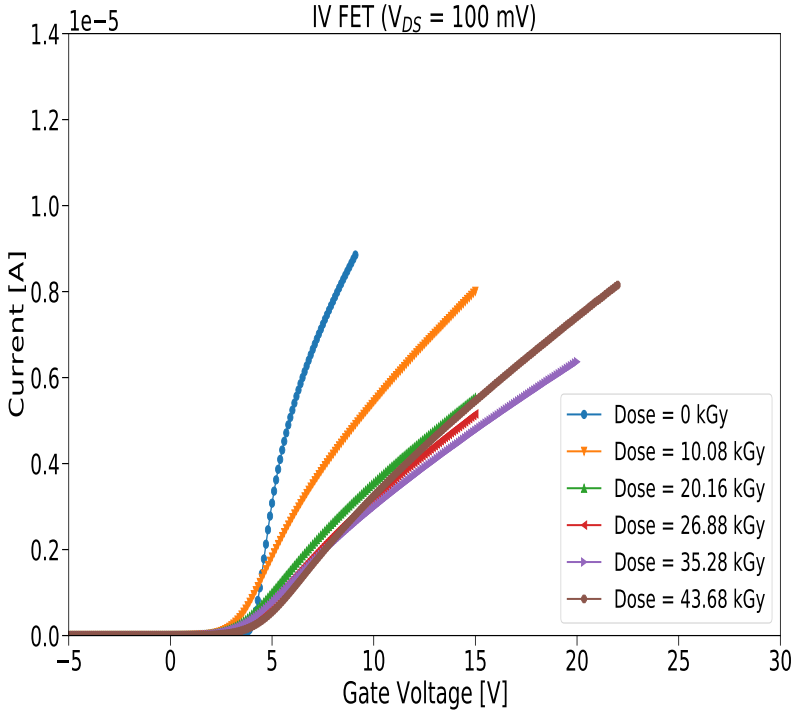

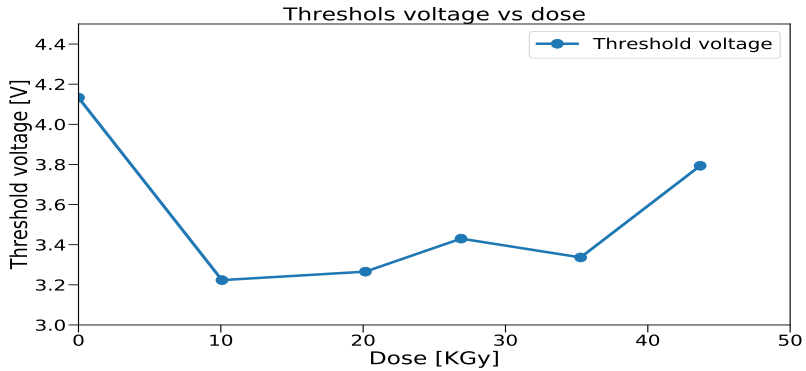

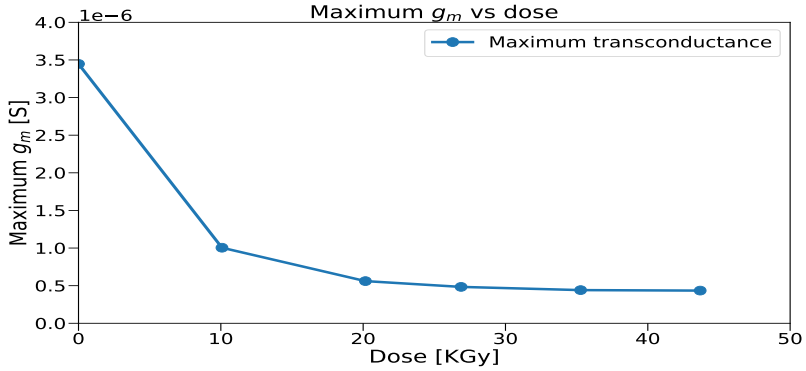

[2] H. Spieler. Semiconductor Detector Systems.2005 .

VDP structures

- VDP p-stop structures
  - Small increase in the sheet resistance of the p-stop.

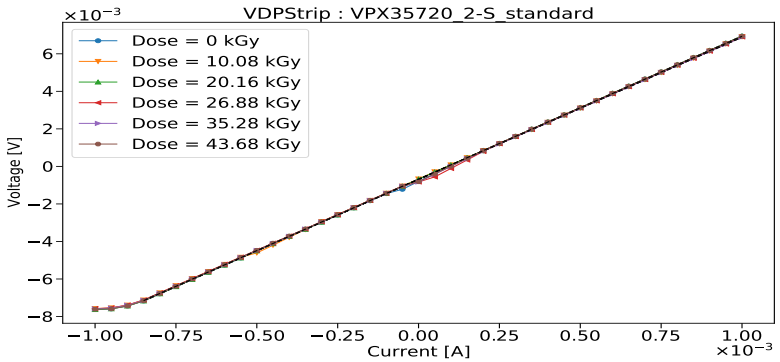

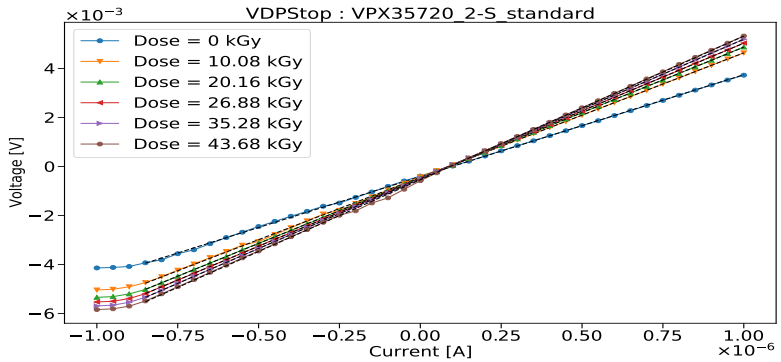

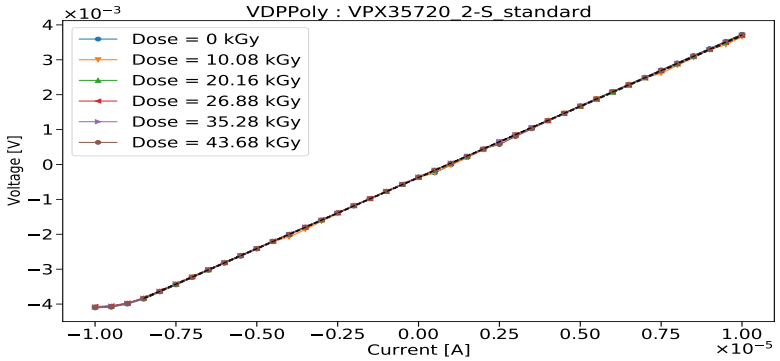

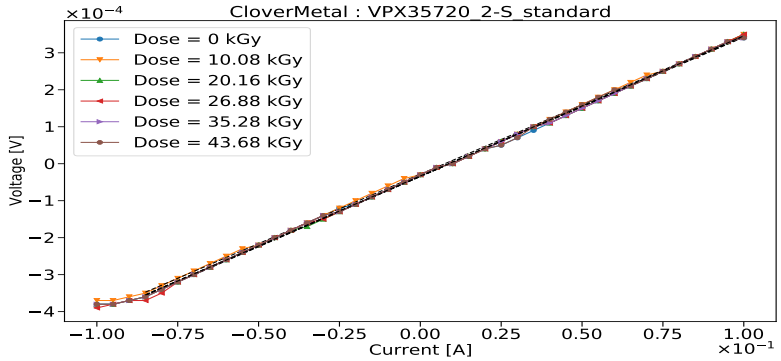

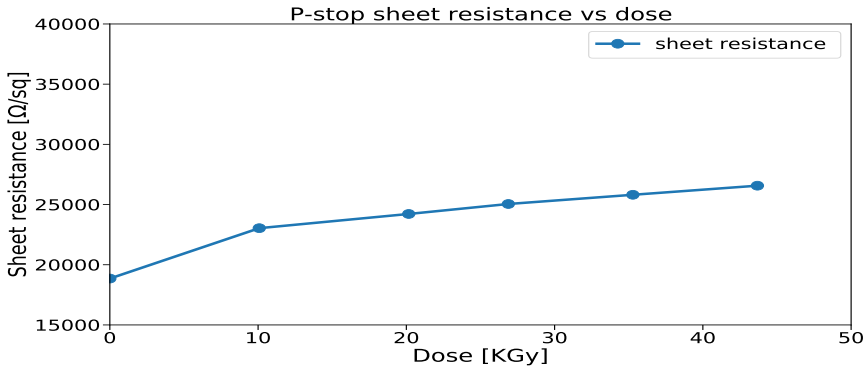

Simulation extras

TCAD simulation of GCD

- TCAD simulations were performed in order to represent the behavior of the GCD before and after irradiation
  - 2D structure with 11 gates (width 60 μm) intertwined with n+ diodes (width 20 μm)
- The model that was used is a modified version of the "New Perugia" model.
- The model combines the *bulk damage* with the *surface damage* effects and was found to represent reasonably well the irradiation tests on MOS capacitors with ^{60}Co γ photons with doses up to 74kGy = 7.4Mrad [3].

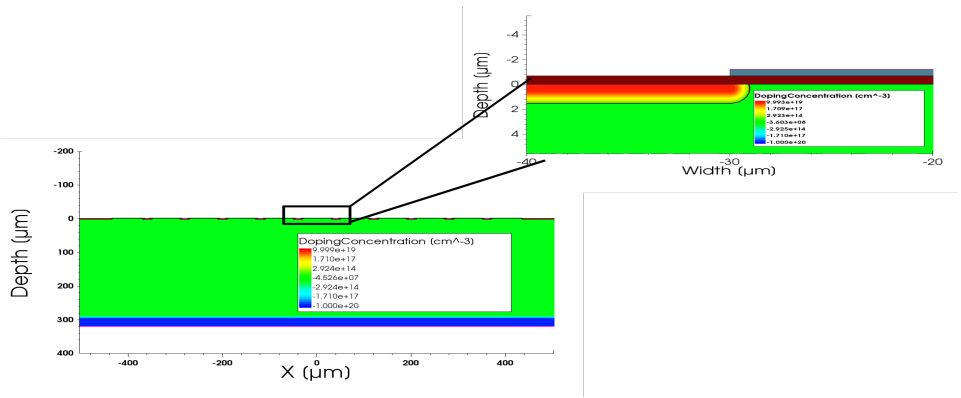

- The model could represent well the unirradiated case

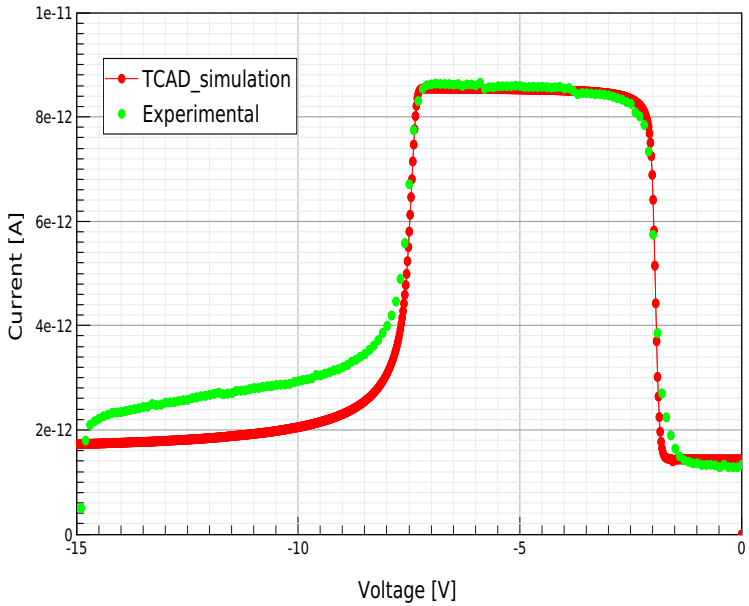

Type	Energy (eV)	Band width (eV)	σ_e (cm^2)	σ_h (cm^2)
Donor	$E_V < E_T < E_V + 0.54$	0.54	1.0×10^{-15}	1.0×10^{-16}
Acceptor	$E_C - 0.58 < E_T < E_c$	0.58	1.0×10^{-16}	1.0×10^{-15}

- [3] P. Asenov, P. Assiouras, A. Boziari, K. Filippou, I. Kazas, A. Kyriakis, D. Loukas, A. Morozzi, F. Moscatelli and D. Passeri, Study of p-type silicon MOS capacitors at HL-LHC radiation levels through irradiation with a cobalt-60 gamma source and a TCAD simulation," JINST **16** (2021) no.06, P06040

TCAD simulation of GCD

- Simulation of the irradiated GCD up to 4.368 Mrad (43.68 kGy)

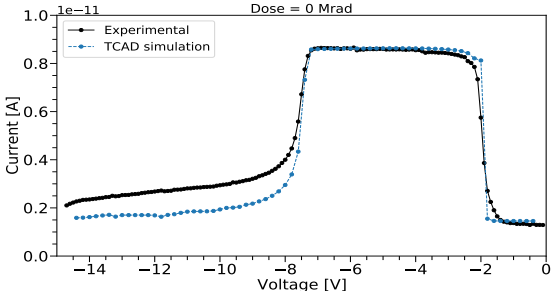

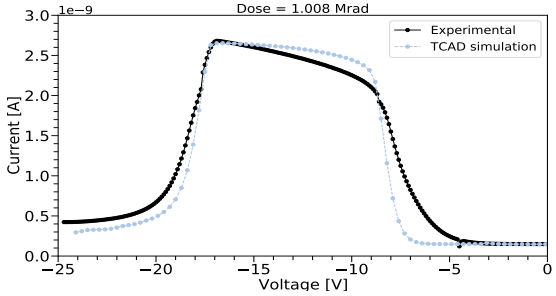

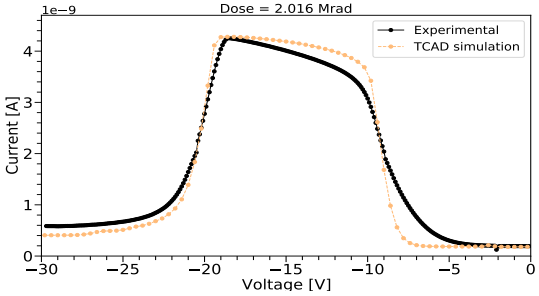

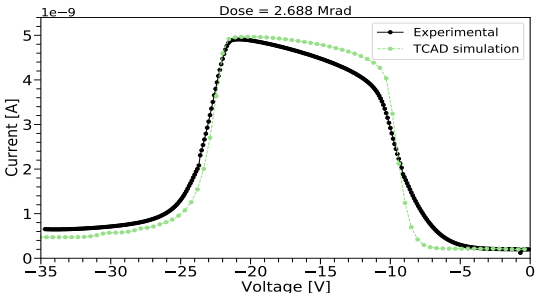

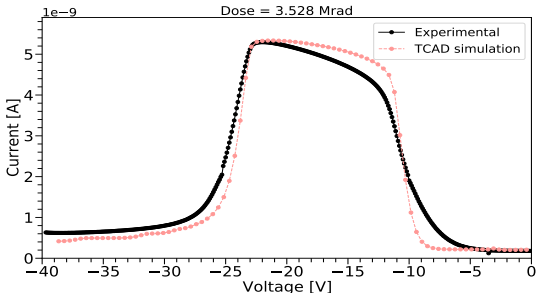

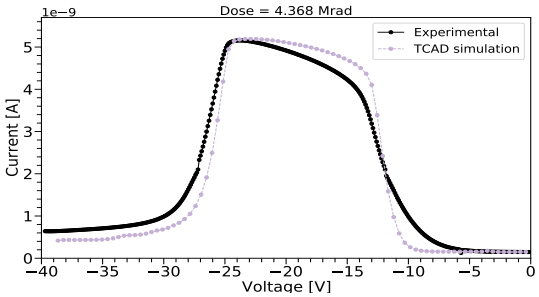

- TCAD input parameters:

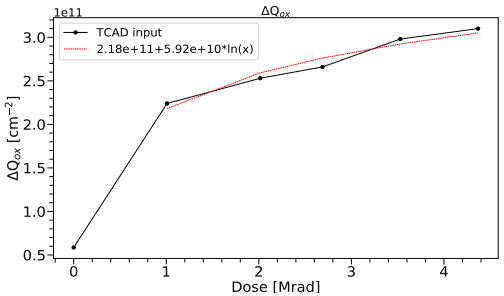

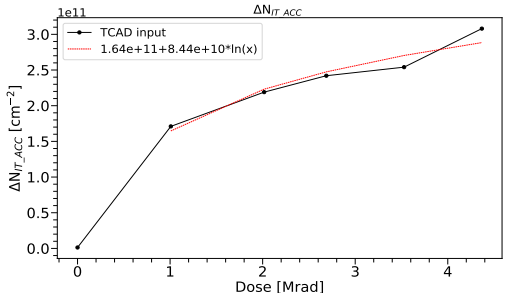

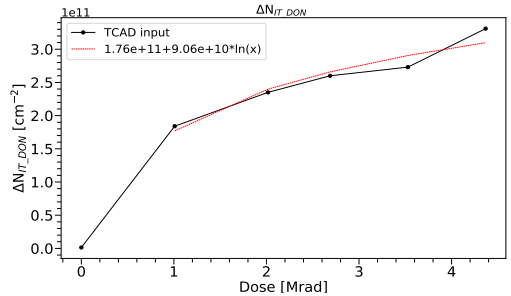

[1] 1 Mrad = 10 kGy

TCAD simulations of MSSD sensors

- A two-dimensional structure was designed, consisting of 5 stips with an n^+p configuration and acive thicknesses of 120 , 200 and 320 μm.
- In an AC-coupled sensor the interstrip capacitance between two strips is calculated by 11

$$C_{int} = C_{Ii-Ij} + C_{Mi-Mj} + C_{Ii-Mj} + C_{Mi-Ij} \qquad (11)$$

- Average accuracy of calculated interstrip capacitance results with the Laplace solver 28% and with TCAD simulations 10 %
- Average accuracy of calculated backplane capacitance with the Laplace solver algorithm 13% and with with TCAD simulations 12 %

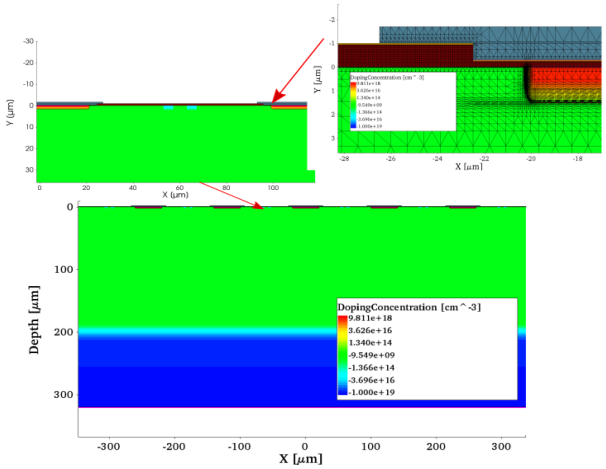

Figure: The 2D structure that was used for simulating the MSSD sensors.

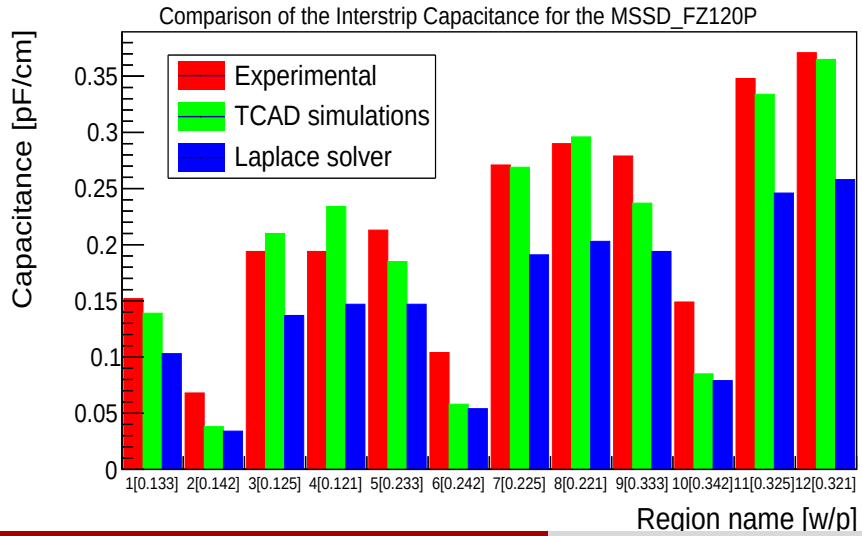

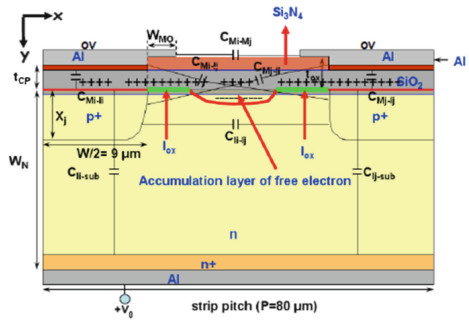

TCAD simulations. Pixel sensors.

- Simulated structures with 9 orthogonal pixels, DC-coupled with a n^+p configuration and an active thickness of 150 μm.

- Simulations have been performed for two different pixel geometries
  - , Pixel size:
    - $50 \times 50\ \mu m^2$
    - $25 \times 100\ \mu m^2$
  - Separation gap varies between 5 μm to 50 μm with a 5 μm step.

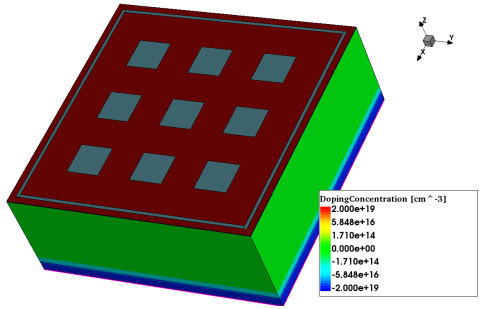

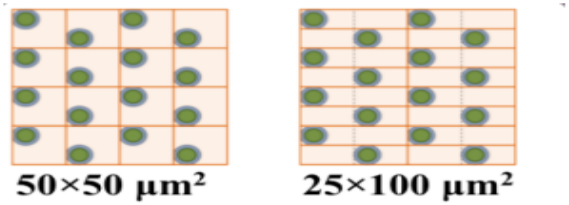

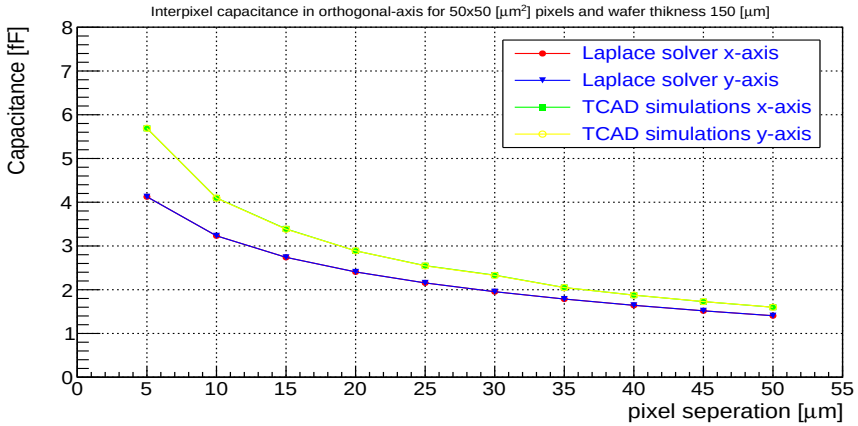

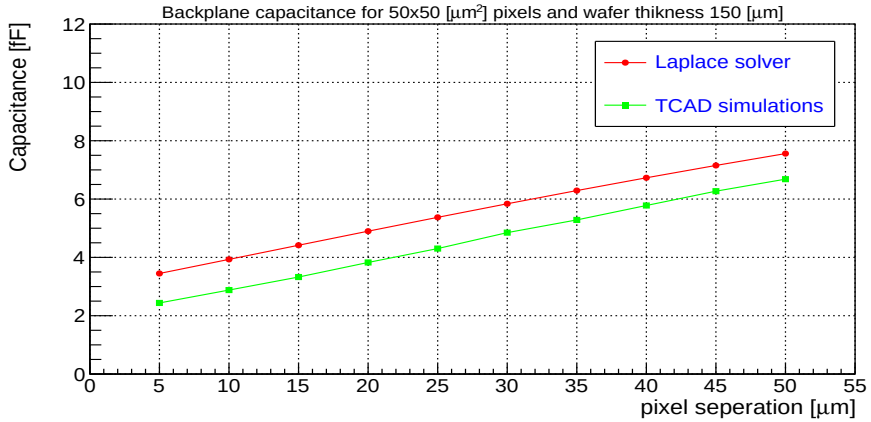

Pixel sensors: Comparison of Laplace solver with TCAD simulations.

- Pixel size : $50 \times 50\ \mu m^2$, Thickness : $150\ \mu m$, Varying separation gap from $5\ \mu m$ to $50\ \mu m$

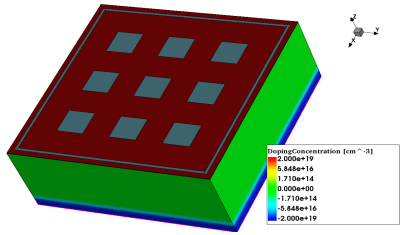

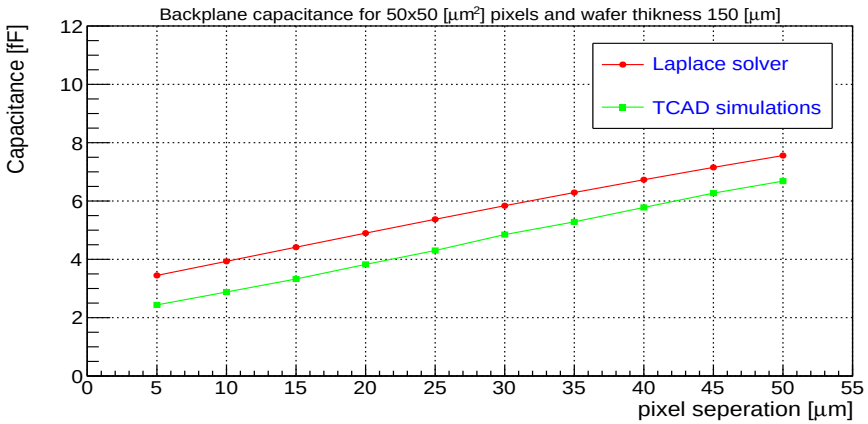

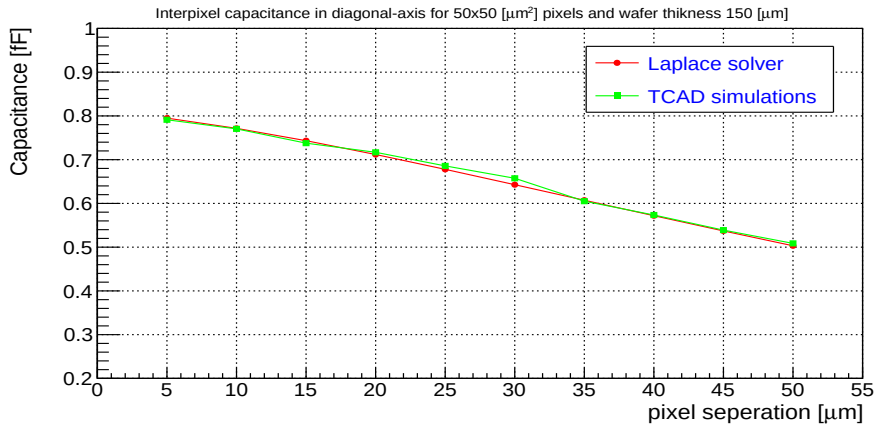

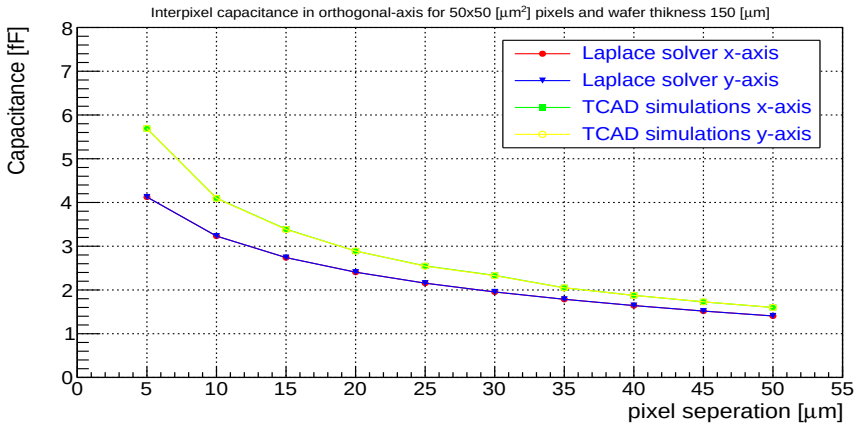

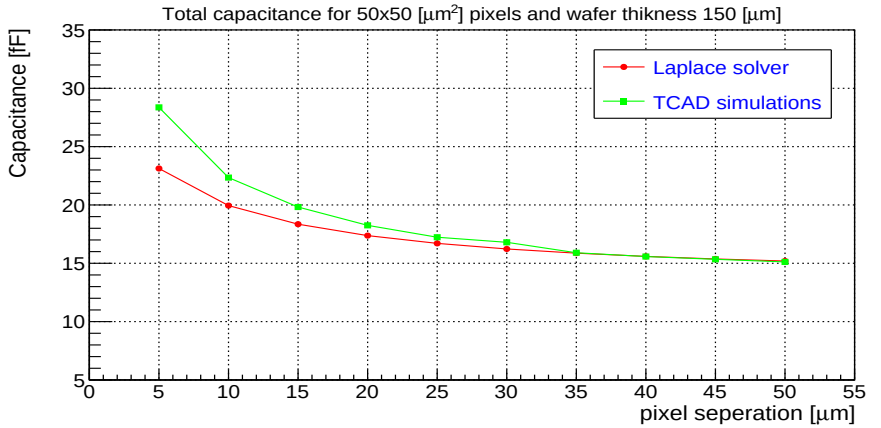

$$C_{tot} = C_{back} + 2.0C_{intx} + 2.0C_{inty} + 4.0C_{diag}$$

Pixel sensors: Comparison of Laplace solver with TCAD simulations.

- Pixel size : $25 \times 100\ \mu m^2$, Thickness : $150\ \mu m$, Varying separation gap from $5\ \mu m$ to $50\ \mu m$

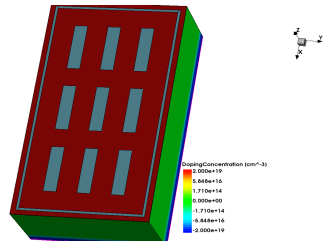

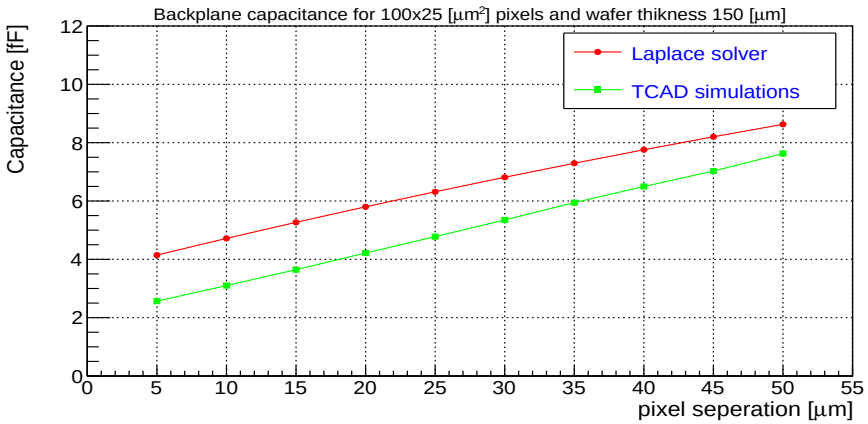

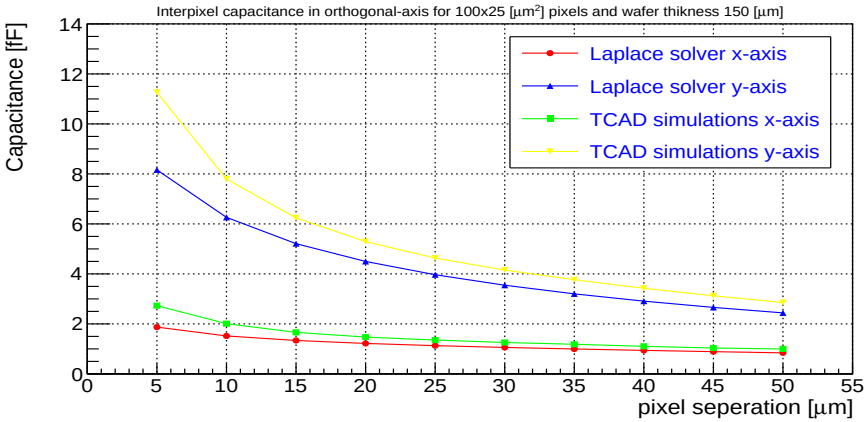

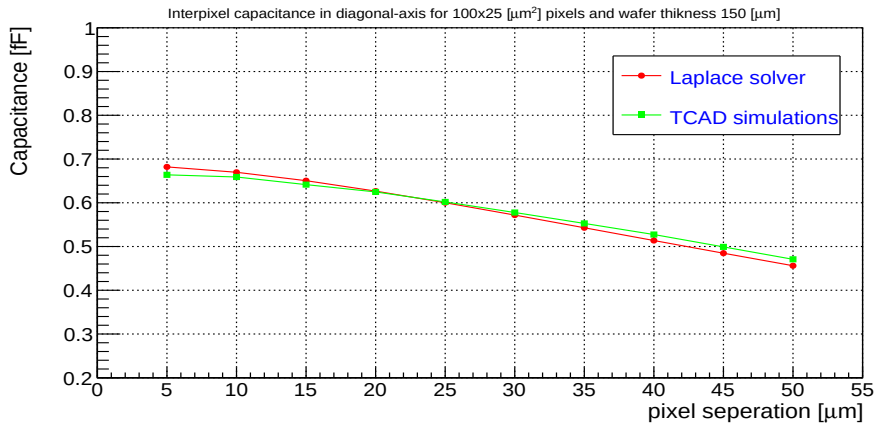

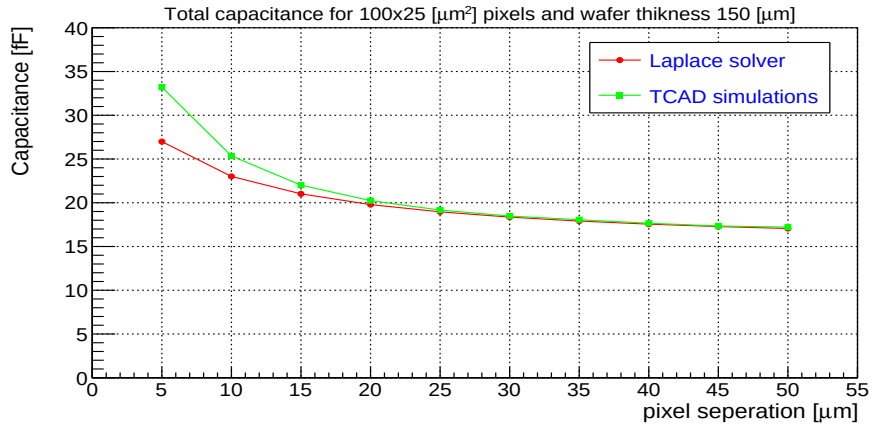

$$C_{tot} = C_{back} + 2.0C_{intx} + 2.0C_{inty} + 4.0C_{diag}$$